A large Late Miocene cetotheriid (Cetacea, Mysticeti) from the Netherlands clarifies the status of Tranatocetidae (#33024)

First submission

Editor guidance

Please submit by **14 Dec 2018** for the benefit of the authors (and your $200 publishing discount).

Structure and Criteria
Please read the 'Structure and Criteria' page for general guidance.

Custom checks
Make sure you include the custom checks shown below, in your review.

Raw data check
Review the raw data. Download from the materials page.

Image check
Check that figures and images have not been inappropriately manipulated.

Privacy reminder: If uploading an annotated PDF, remove identifiable information to remain anonymous.

Files

Download and review all files from the materials page.

12 Figure file(s)
2 Table file(s)
1 Raw data file(s)

Custom checks

New species checks

- Have you checked our new species policies?
- Do you agree that it is a new species?
- Is it correctly described e.g. meets ICZN standard?

Structure your review

The review form is divided into 5 sections. Please consider these when composing your review:

1. **BASIC REPORTING**
2. **EXPERIMENTAL DESIGN**
3. **VALIDITY OF THE FINDINGS**
4. General comments
5. Confidential notes to the editor

You can also annotate this PDF and upload it as part of your review

When ready submit online.

Editorial Criteria

Use these criteria points to structure your review. The full detailed editorial criteria is on your guidance page.

BASIC REPORTING

- Clear, unambiguous, professional English language used throughout.
- Intro & background to show context. Literature well referenced & relevant.
- Structure conforms to PeerJ standards, discipline norm, or improved for clarity.
- Figures are relevant, high quality, well labelled & described.
- Raw data supplied (see PeerJ policy).

EXPERIMENTAL DESIGN

- Original primary research within Scope of the journal.
- Research question well defined, relevant & meaningful. It is stated how the research fills an identified knowledge gap.
- Rigorous investigation performed to a high technical & ethical standard.
- Methods described with sufficient detail & information to replicate.

VALIDITY OF THE FINDINGS

- Impact and novelty not assessed. Negative/inconclusive results accepted. *Meaningful* replication encouraged where rationale & benefit to literature is clearly stated.
- Data is robust, statistically sound, & controlled.
- Speculation is welcome, but should be identified as such.
- Conclusions are well stated, linked to original research question & limited to supporting results.

Standout reviewing tips

The best reviewers use these techniques

Tip	*Example*
Support criticisms with evidence from the text or from other sources	*Smith et al (J of Methodology, 2005, V3, pp 123) have shown that the analysis you use in Lines 241-250 is not the most appropriate for this situation. Please explain why you used this method.*
Give specific suggestions on how to improve the manuscript	*Your introduction needs more detail. I suggest that you improve the description at lines 57- 86 to provide more justification for your study (specifically, you should expand upon the knowledge gap being filled).*
Comment on language and grammar issues	*The English language should be improved to ensure that an international audience can clearly understand your text. Some examples where the language could be improved include lines 23, 77, 121, 128 – the current phrasing makes comprehension difficult.*
Organize by importance of the issues, and number your points	*1. Your most important issue* *2. The next most important item* *3. …* *4. The least important points*
Please provide constructive criticism, and avoid personal opinions	*I thank you for providing the raw data, however your supplemental files need more descriptive metadata identifiers to be useful to future readers. Although your results are compelling, the data analysis should be improved in the following ways: AA, BB, CC*
Comment on strengths (as well as weaknesses) of the manuscript	*I commend the authors for their extensive data set, compiled over many years of detailed fieldwork. In addition, the manuscript is clearly written in professional, unambiguous language. If there is a weakness, it is in the statistical analysis (as I have noted above) which should be improved upon before Acceptance.*

A large Late Miocene cetotheriid (Cetacea, Mysticeti) from the Netherlands clarifies the status of Tranatocetidae

Felix Georg Marx Corresp., [1, 2, 3] , **Klaas Post** [4] , **Mark Bosselaers** [2, 5] , **Dirk K. Munsterman** [6]

[1] Geology, Université de Liège, Liège, Belgium
[2] Directorate of Earth and History of Life, Royal Belgian Institute of Natural Sciences, Brussels, Belgium
[3] Palaeontology, Museums Victoria, Melbourne, Victoria, Australia
[4] Natuurhistorisch Museum, Rotterdam, The Netherlands
[5] Zeeland Royal Society of Sciences, Middelburg, The Netherlands
[6] Netherlands Institute of Applied Geoscience TNO, Utrecht, The Netherlands

Corresponding Author: Felix Georg Marx
Email address: felix.marx@naturalsciences.be

Cetotheriidae are a group of small baleen whales (Mysticeti) that evolved alongside modern rorquals. They once enjoyed a nearly global distribution, but then largely went extinct during the Plio-Pleistocene. After languishing as a wastebasket taxon for more than a century, the concept of Cetotheriidae is now well established. Nevertheless, the clade remains notable for its variability, and its scope remains in flux. In particular, the recent referral of several traditional cetotheriids to a new and seemingly unrelated family, Tranatocetidae, has created major phylogenetic uncertainty. Here, we describe a new species of *Tranatocetus*, the type of Tranatocetidae, from the Late Miocene of the Netherlands. The new material clarifies several of the traits previously ascribed to this genus, and reveals distinctive auditory and mandibular morphologies suggesting cetotheriid affinities. This interpretation is supported by a large phylogenetic analysis, which mingles cetotheriids and tranatocetids within a unified clade. As a result, we suggest that both groups should be reintegrated into the single family Cetotheriidae.

A large Late Miocene cetotheriid (Cetacea, Mysticeti) from the Netherlands clarifies the status of Tranatocetidae

Felix G. Marx[1–3], Klaas Post[4], Mark Bosselaers[2,5] and Dirk K. Munsterman[6]

[1]Department of Geology, University of Liège, B18, Quartier Agora, 14 Allée du 6 Août, 4000 Liège, Belgium.
Corresponding author: felix.marx@naturalsciences.be

[2]Directorate of Earth and History of Life, Royal Belgian Institute of Natural Sciences, Brussels, Belgium.

[3]Geosciences, Museum Victoria, Melbourne, Australia.

[4]Natuurhistorisch Museum Rotterdam, Rotterdam, the Netherlands

[5]Zeeland Royal Society of Sciences, Middelburg, the Netherlands.

[6]Netherlands Institute of Applied Geoscience TNO – National Geological Survey, Utrecht, the Netherlands.

Abstract: Cetotheriidae ~~are~~ a group of small baleen whales (Mysticeti) that evolved alongside modern rorquals. They once enjoyed a nearly global distribution, but then largely went extinct during the Plio-Pleistocene. After languishing as a wastebasket taxon for more than a century, the concept of Cetotheriidae is now well established. Nevertheless, the clade remains notable for its variability, and its scope remains in flux. In particular, the recent referral of several traditional cetotheriids to a new and seemingly unrelated family, Tranatocetidae, has created major phylogenetic uncertainty. Here, we describe a new species of *Tranatocetus*, the type of Tranatocetidae, from the Late Miocene of the Netherlands. The new material clarifies several of the traits previously ascribed to this genus, and reveals distinctive auditory and mandibular morphologies suggesting cetotheriid affinities. This interpretation is supported by a large phylogenetic analysis, which mingles cetotheriids and tranatocetids within a unified clade. As a result, we suggest that both groups should be reintegrated into the single family Cetotheriidae.

Keywords: baleen whale, phylogeny, systematics, evolution, body size

INTRODUCTION

Cetotheriids are one of three major branches of modern baleen whales, alongside right whales (Balaenidae) and rorquals (Balaenopteridae). The family is first recorded during the Middle Miocene (Gol'din 2018), but its roots likely stretch further back in time (Marx & Fordyce 2015). Late Miocene cetotheriids were speciose and attained a nearly global distribution, with records from the North Atlantic (Bisconti 2015; Marx et al. 2016; Whitmore & Barnes 2008), the Paratethys (Gol'din & Startsev 2017), and both the North (El Adli et al. 2014; Kellogg 1929; Saita et al. 2011; Tanaka et al. 2018b; Tanaka & Watanabe 2018) and eastern South Pacific (Bouetel & de Muizon 2006; Marx et al. 2017).

This taxonomic diversity was accompanied by notably disparity, giving rise to at least three distinct morphotypes: (i) Cetotheriinae, a group of small-bodies species closely related to the eponymous *Cetotherium*, and apparently endemic to the Paratethys (Gol'din & Startsev 2017); (ii) a second group of small-bodied whales that inhabited the North Atlantic and North Pacific, and came to the fore during the Pliocene (Boessenecker 2011; El Adli et al. 2014; Tanaka et al. 2018b; Tanaka & Watanabe 2018; Whitmore & Barnes 2008); and (iii) a possibly para- or even polyphyletic assemblage of species comprising *Herentalia*, *Metopocetus*, and *Piscobalaena* (Bouetel & de Muizon 2006; Gol'din & Steeman 2015; Marx et al. 2017).

Beyond these morphotypes, the scope of the family remains in doubt. This is partly because of the proposed inclusion of *Cephalotropis* and neobalaenines, which has proved controversial (Bisconti 2015; El Adli et al. 2014; Fordyce & Marx 2013; Gol'din & Steeman 2015; Marx & Fordyce 2016); and partly because of the recent referral of several presumed cetotheriids, such as '*Cetotherium*' *megalophysum* and '*Metopocetus*' *vandelli*, to the new and seemingly unrelated family Tranatocetidae (Gol'din & Steeman 2015).

Tranatocetidae was defined based on *Tranatocetus argillarius*, known only from the Late Miocene clay pit of Gram, Denmark. *Tranatocetus* indeed stands out for its large size, relative to cetotheriids, but its interpretation is severely hampered by the poor preservation of the available material. In particular, crushing and breakage have affected all of the holotype, obliterating details of the otherwise highly diagnostic ear region and necessitating extensive reconstructions of the mandible (Gol'din & Steeman 2015; Roth 1978).

Here, we report a second species of *Tranatocetus*, based on two Late Miocene fossils dredged from the bottom of the Western Scheldt (the Netherlands). The new specimens preserve crucial details that are absent in the type material of *T. argillarius*, and thus offer a perfect opportunity to test the idea that Tranatocetidae and Cetotheriidae indeed form separate clades.

MATERIAL AND METHODS

Collection, preparation, body size and phylogenetic analysis

The specimens described here were trawled from the bottom of the Western Scheldt (the Netherlands) during NMR expeditions 2014-3 and 2015-1 (Fig. 1). Both fossils were embedded in a matrix of hard glauconitic sandstone, and prepared mechanically. For the description, morphological terminology follows Mead & Fordyce (2009), unless indicated. Photographs of the specimens were digitally stacked in Photoshop CS6.

Total body length was estimated based on bizygomatic width, using the stem balaenopteroid equation of Pyenson & Sponberg (2011), and the general mysticete equation of ~~Lambert et al. (Lambert et al. 2010)~~. To establish evolutionary relationships, we coded our new material, as well as *Tranatocetus argillarius* and the recently described Middle Miocene cetotheriid *Ciuciulea davidi* (Gol'din & Steeman 2015; Gol'din 2018), into a slightly modified version of the phylogenetic matrix of Fordyce & Marx (2018). The analysis was run in MrBayes 3.2.6, on the Cyberinfrastructure for Phylogenetic Research (CIPRES) Science Gateway (Miller et al. 2010), using the same settings as in Fordyce and Marx (2018). The full cladistic matrix is available as online supplementary material.

Age determination

Matrix samples from the more complete specimen (NMR 9991-16680) were prepared at Palynological Laboratory Services (PLS, UK) using standard sample processing procedures, which involve HCl and HF treatment, heavy liquid separation, and sieving over a 15µm mesh sieve. The organic residue was mounted with glycerine-gelatine on microscopic slides. Two microscopic slides were made: one carrying non-oxidized kerogen, and one on which the organic residue was slightly oxidized with HNO_3 to concentrate the palynomorphs and reduce ‘Structureless Organic Matter’.

Palynological analysis was carried out at the Geological Survey of the Netherlands (TNO). We counted the first 200 sporomorphs (pollen and spores) and dinoflagellate cysts, and thereafter scanned for any rarer dinocyst species. Major miscellaneous categories (e.g. marine acritarchs, test linings of foraminifers and the brackish alga *Botryococcus*) were calculated separately. Age interpretations were based on the first and last occurrences of dinoflagellate cysts, using the dinozones of Munsterman & Brinkhuis (2004) recalibrated to Ogg et al. (2016). Dinoflagellate cyst taxonomy follows the 'Lentin and Williams index' (Williams et al. 2017).

Nomenclatural acts

The electronic version of this article in Portable Document Format (PDF) will represent a published work according to the International Commission on Zoological Nomenclature (ICZN), and hence the new names contained in the electronic version are effectively published under that Code from the electronic edition alone. This published work and the nomenclatural acts it contains have been registered in ZooBank, the online registration system for the ICZN. The ZooBank LSIDs (Life Science Identifiers) can be resolved and the associated information viewed through any standard web browser by appending the LSID to the prefix http://zoobank.org/. The LSID for this publication is: urn:lsid:zoobank.org:pub:D39ACC32-687F-4C95-9CD8-A2B17B2DBAFC. The online version of this work is archived and available from the following digital repositories: PeerJ, PubMed Central and CLOCKSS.

Institutional abbreviations

GMUC, Geological Museum of the University of Copenhagen, Denmark; MNHN, Museum National d`Histoire Naturelle, Paris, France; NMR, Natuurhistorisch Museum Rotterdam, the Netherlands; USNM, United States National Museum of Natural History, Washington DC, USA.

RESULTS

Systematic palaeontology

Cetacea Brisson, 1762

Neoceti Fordyce and de Muizon, 2001

Mysticeti Gray, 1864

Chaeomysticeti Mitchell, 1989

Cetotheriidae Brandt, 1872

Tranatocetus Gol'din and Steeman, 2015

Type species. *Tranatocetus argillarius* (Roth, 1978)

Emended diagnosis. Large cetotheriid sharing with other members of the family the presence of an enlarged compound posterior process of the tympanoperiotic [hereafter, compound posterior process], an enlarged paroccipital concavity extending on to the compound posterior process, elongate, medially convergent ascending processes of the maxillae, a supraoccipital shield whose tip does not extend beyond the apex of the zygomatic process of the squamosal, and a posteriorly projected angular process of the mandible bearing a well-defined fossa for the medial pterygoid muscle. Further shares with all cetotheriids except *Cephalotropis* and *Joumocetus* the posterior telescoping of the ascending process of the maxilla up to, or beyond, the level of the parietal. Differs from all described cetotheriids in its larger size, in having a flattened platform located inside the posterodorsal corner of the mandibular fossa, and in having a mandibular condyle that does not markedly rise above the level of the mandibular neck. Further differs from all cetotheriids except *Herentalia* in having a notably elongate anterior process of the periotic; from all cetotheriids except *Metopocetus* in having a reduced lateral tuberosity; from all cetotheriids except *Herentalia*, *Metopocetus* and *Piscobalaena* in having a sharp cranial rim surrounding the proximal opening of the facial canal; from *Brandtocetus*, *Cetotherium*, *Kurdalagonus* and *Mithridatocetus* in having a larger posteroventral flange of the compound posterior process that completely floors the facial sulcus, a tympanic bulla that is less squared and narrower anteriorly than posteriorly (in ventral view), a more elongate ascending process of the maxilla, and a more gracile zygomatic process of the squamosal; from *Cephalotropis*, *Ciuciulea* and *Joumocetus* in lacking a long exposure of the parietal on the vertex; from *Cephalotropis* in having a proportionally larger bulla, and a better-developed posteroventral flange of the compound posterior process; from *Herpetocetus* and *Piscobalaena* in having a squamosal cleft; from *Piscobalaena* in having a sharper vomerine crest; from *Herpetocetus* in lacking a postparietal foramen; from '*Cetotherium*' *megalophysum* in having a distally larger compound posterior process with a better-developed posteroventral flange, and a more concave supraoccipital shield;

from *Metopocetus* in having a more elongate ascending process of the maxilla, a narrower posterior portion of the nasal, and a smaller tympanohyal; and from *Herentalia* in having a more pointed apex of the supraoccipital shield and a better-developed external occipital crest.

Tranatocetus maregermanicum, sp. nov.

Figures 2–8

LSID. urn:lsid:zoobank.org:act:499F1C5C-3C3F-48A9-AD97-AF19F99DE886

Holotype. NMR9991-16680, partial cranium comprising the braincase and ear bones, posterior portions of both mandibles, a fragmentary atlas, and two thoracic vertebrae.

Paratype. NMR9991-16681, basicranium, right periotic, atlas, and seventh cervical vertebra.

Locality and horizon. Both fossils were recovered from the Breda Formation, exposed at site 6d (N51°21’56.9”, E3°54’25.1”) of Post & Reumer (2016). Assemblages from the associated matrix are relatively rich in marine dinoflagellate cysts, but include only around 10% of sporomorphs (~~Table S1)~~. The latter mostly consist of bisaccate pollen (71%), which are relatively buoyant and, along with the abundance of dinocysts, indicate a distal position from the coast. The most abundant dinocyst genus is *Spiniferites* (39% of the total dinocyst sum), which preferentially occurs in open marine conditions. However, the temperate–tropical, inner neritic *Barssidinium graminosum* and the coastal *Lingulodinium machaerophorum* are also well-represented (24% and 6%, respectively), suggesting overall neritic conditions.

Enneadocysta pectiniformis and *Glaphyrocysta* spp. are reworked from the Oligocene or older intervals. Among the age-diagnostic taxa, *Hystrichosphaeropsis obscura* last occurs in Zone SNSM14 (ca. 7.5 Ma), and defines the DN9 Zone of de Verteuil & Norris (1996) and the *Hystrichosphaeropsis obscura* Zone of Dybkjaer and Piasecki (2010). The presence of *Selenopemphix armageddonensis* confirms a dating no older than late Tortonian. The first occurrence of this species has variously been placed at either 7.5 Ma (Zone DN10; de Verteuil & Norris 1996; Dybkjær & Piasecki 2010), or at 9 Ma in equatorial areas (Williams et al. 2004). In Belgium, it has been recorded from the Kasterlee Formation (Louwye & de Schepper 2010), whereas in the Netherlands it extends to the top of Zone SNSM13, which dates to approximately

8.1 Ma (well Groote Heide). Together, these observations constrain the current assemblage to Zone SNSM14, Late Miocene, ca. 8.1–7.5 Ma (Munsterman & Brinkhuis 2004, recalibrated to Ogg et al. 2016).

Diagnosis. Shares with *Tranatocetus argillarius* its large overall size, slender ascending processes of the maxillae that are situated centrally on a triangular platform formed by the frontals, a narrow but continuous exposure of the nasals between the ascending processes of the maxillae, the lack of an external occipital crest, a bulbous exoccipital, an elongate anterior process of the periotic lacking a lateral tuberosity, a large paroccipital concavity, a large mandibular fossa housing a flattened platform in its posterodorsal corner, a deep subcondylar furrow, and a mandibular condyle that does not markedly rise above the level of the mandibular neck. Differs from *T. argillarius* in being slightly larger, in having a more anterolaterally directed base of the supraorbital process of the frontal, a more robust zygomatic process of the squamosal, relatively larger occipital condyles projecting posteriorly beyond the posterior apex of the nuchal crest, a vomerine crest extending posteriorly far beyond the level of the subtemporal crest, and a sharper, dorsally convex ventral border of the mandibular foramen.

Etymology. After the Latin name of the North Sea, *Mare Germanicum*, which *Tranatocetus* once inhabited.

Description

Overview. The posterior portion of the skull of NMR9991-16680 is nearly complete, except for the zygomatic processes of the squamosals (Fig. 2). The surface of the vertex is somewhat eroded, and the rostral bones have become detached and have slid forwards along their respective sutures. The rostrum and the supraorbital processes of the frontals are mostly missing. Ventrally, the posterior halves of both mandibles are nearly *in situ*. Anteriorly, the mandibles and the vomer are truncated by a continuous oblique fracture, suggesting that the specimen was broken, and its anterior half lost, during dredging. Posteriorly, the atlas and a single thoracic vertebra still adhere to the skull. A second thoracic vertebra was removed during preparation. NMR9991-16681 consists of a well-preserved basicranium, with the right periotic *in situ* but partially obscured (Fig. 3). See Table 1 for measurements of both specimens.

Maxilla, premaxilla and nasal. In dorsal view, the ascending process of the maxilla is narrow, parallel-sided, and elongate (Fig. 1). Posteriorly, the ascending processes converge, but appear to remain separated by a thin sliver of nasal. The premaxilla is missing but, judging from the lack of space between the nasal and the maxilla, did not contact the frontal on the vertex. Except for a narrowly exposed section between the posterior maxillae, the nasals are lost and/ or obscured by sediment. In lateral view, the maxilla gently descends from the vertex, suggesting an overall concave facial profile (Figs 4, 5). The posteriormost portion of the maxilla extends posteriorly beyond the level of the coronal suture.

Vomer. In anterior view, the fractured vomer is V-shaped in cross section and floors the mesorostral groove (Fig. 5). In ventral view, the ventral portion of the vomer gradually flares at the level of the temporal fossa to form a lozenge-shaped platform (Fig. 6). Posterior to this platform, the tall but rounded vomerine crest ascends towards the braincase, and eventually merges with the plate-like posteriormost portion of the vomer that separates the pharyngeal crests.

Frontal. In dorsal view, the frontal is nearly excluded from the vertex, and forms a V-shaped suture with the parietal (Fig. 2). There is no obvious narial process. A well-defined orbitotemporal crest originates on the vertex, and from there runs close and nearly parallel to the posterior border of the supraorbital process. Medially, this crest is separated from the ascending process of the maxilla by an anteriorly widening triangular basin. In anterior view, the base of the supraorbital process is descending gradually from the vertex, with its dorsal border being notably concave (Fig. 5).

Parietal. In dorsal view, the parietal appears to be virtually excluded from the vertex, but it (or the interparietal) still likely contributes to the apex of the supraoccipital shield (Fig. 2). Anteriorly, a nearly vertical, triangular 'wing' of the parietal overrides the posteromedial portion of the frontal and underlaps the orbitotemporal crest (Fig. 4). Unlike in *Herentalia*, *Metopocetus* and *Piscobalaena*, the anterodorsal border of the parietal does not flare laterally, and hence does not 'buttress' the vertex. The parieto-squamosal suture is sigmoidal: after descending from the nuchal crest, it turns first anterolaterally and then anteromedially, before terminating at the presumed position of the alisphenoid. Along the suture, the parietal and squamosal slightly bulge into the temporal fossa. There is no tubercle at the junction of the parieto-squamosal suture with the nuchal crest, and no postparietal foramen (Fig. 4).

Squamosal. In dorsal view, the temporal fossa is wider than long (Fig. 2). The squamosal fossa is elongate, and approximately as long as the temporal fossa is wide. The base of the zygomatic process is oriented somewhat anterolaterally, and bears a gently rounded supramastoid crest. On the right, there is a low but clearly defined squamosal prominence. The posterior apex of the nuchal crest is located anterior to the level of the occipital condyles. A squamosal cleft is present and extends laterally from the presumed location of the alisphenoid. There is no squamosal crease.

In ventral view, the base of the postglenoid process is oriented transversely, with no obvious twisting (Figs 2, 6). The glenoid fossa is smooth and not visibly offset from the surrounding bone. The fossa for the sigmoid process of the tympanic bulla is indistinct. Medially, the postglenoid is confluent with a low anterior meatal crest delimiting the proximal portion of the external acoustic meatus. The posterior meatal crest descends along the anterior face of the compound posterior process, and extends laterally on to the posterior face of the postglenoid process. The falciform process is robust, hook-shaped and separated from the spinous process by an approximately rectangular fenestra, similar to *Metopocetus.* The foramen pseudovale is almost entirely surrounded by the squamosal, except for a narrow sliver of pterygoid that contributes to its anterior border.

In lateral view, the zygomatic process is robust and approximately as tall as it is wide transversely (Fig. 5). The postglenoid process is triangular, with a vertical posterior face and a posteroventrally oriented anterior border. Anterodorsal to the compound posterior process, and immediately below the supramastoid crest, there is a large fossa for the sternocephalicus that partially excavates the supramastoid crest. In posterior view, the postglenoid process is approximately parabolic in outline, and descends ventrally well below the level of the exoccipital.

Alisphenoid. The alisphenoid remains obscured by matrix, but a depression in the temporal wall, between the parietal dorsally and the squamosal ventrally, marks its likely position, and suggest that the alisphenoid may have contributed to the orbital fissure (Fig. 4).

Supraoccipital, exoccipital, basioccipital. In dorsal view, the supraoccipital is sharply triangular, and extends anteriorly beyond the level of the subtemporal crest (Fig. 2). The nuchal crest is oriented dorsolaterally but does not overhang the temporal fossa. Between the nuchal crests, the supraoccipital shield is initially flattened near its apex, but then becomes moderately concave transversely. Its surface is largely eroded, but seems to have lacked a well-developed external occipital crest. The exoccipital is robust, anteroposteriorly thickened, and extends posteriorly well beyond the level of the occipital condyles. The condyles themselves are robust and lack a distinct neck.

In posterior view, the foramen magnum is rounded, and approximately half as high as the occipital condyles (Fig. 3). The paroccipital process is concave ventrally, slightly offset from the more lateral portion of the exoccipital by a blunt notch, and descends to approximately the same level as the basioccipital crest.

In ventral view, the basioccipital crest is robust and approximately triangular (Figs 6, 7). The jugular notch is relatively wide and oriented ventrolaterally. The paroccipital concavity is enormous, and medially excavates the bony wall that separates it from the jugular notch (Fig. 7). The posterior border of the paroccipital cavity is thin, but then markedly thickens laterally and protrudes outwards. Anteriorly, the roof of the paroccipital concavity is uneven, with a noticeably raised centre; the anterior border of the concavity closely approximates the compound posterior process.

Periotic. In anterior view, the anterior process is curved dorsoventrally, with the medial face being somewhat concave and the outer surface convex. In medial view, the anterior process is approximately squared, but sediment obscures its precise outline.

In ventral view, the anterior process is robust, elongate, and more than 1.5 times as long as the pars cochlearis (Fig. 7). The anterior process and body of the periotic remain nearly constant in width anteroposteriorly, with no visible hypertrophy. The ventral border of the anterior process bears a sharp keel, which posteriorly terminates in the fused anterior pedicle of the tympanic bulla. The lateral tuberosity and anteroexternal sulcus are indistinct. The pars cochlearis is globular, and anterodorsally bears a shallow depression. Anteroventral to the pars cochlearis, there is a short, robust ridge for the tensor tympani. The mallear fossa is deep, but poorly defined. Posterior to the mallear fossa, there is a bulbous, low squamosal flange.

The compound posterior process is enlarged, plug-like, and clearly exposed on the outer skull wall (Fig. 7). Its distal surface is flattened, and offset from the ventral face of the process and the facial sulcus by a clear angle. The facial sulcus is floored by a large posteroventral flange (sensu Marx et al. 2016), which widens and thickens externally, and forms the anterior extension of the paroccipital concavity. Medially, the thickened outer portion of the posteroventral flange is delimited by a notch, presumably marking the position of the posteroventral sulcus (sensu Marx et al. 2017). Anteriorly, the expanded paroccipital concavity is delimited by a robust, posteroventrally curving anteroventral flange.

Tympanic bulla. The right bulla is *in situ* and partially covered by the mandible (Figs 6, 7). In ventral view, the anterior portion of the tympanic bulla is somewhat narrower than its posterior half. The ventral surface of the bulla is transversely convex throughout. In lateral view, the lateral furrow is approximately vertical. The sigmoid process is straight and lacks a distinct ventral border. The conical process is convex dorsally, and located entirely posterior to the sigmoid process. In posterior view, there are well-developed inner and outer posterior prominences, separated from each other by a shallow median furrow. As in other crown mysticetes, the bulla has rotated medially, so that the main ridge faces medially towards the basioccipital crest. Other morphological details remain obscured by the mandible.

Mandible. In medial view, the coronoid process is low and broadly triangular (Fig. 8). The mandibular foramen is tall dorsoventrally, thus forming a mandibular fossa; it is framed by a robust ventral border, and anteriorly reaches the level of the coronoid process. The angular process is massive, projects posteriorly beyond the level of the mandibular condyle, and bears an elongate fossa for the attachment of the medial pterygoid muscle. The subcondylar furrow is deep and well defined. The medial surface of the condyle is somewhat excavated, and forms a platform occupying the posterodorsal corner of the mandibular fossa.

In lateral view, the condyle is approximately aligned with mandibular neck. Its articular surface points largely posteriorly, but is confluent with a thickened, posterodorsally oriented ridge (Fig. 8). Anterior to the condyle, the lateral surface of the mandible is excavated by a deep fossa for the attachment of the deep masseter muscle. The subcondylar furrow is visible as a distinct notch in the posterior profile of the ramus, but does not extend on to its lateral surface. Lateral to the subcondylar furrow, the condyle and angular process are connected by a sharp crest. The angular process gently descends below the level of the ventral border of the mandibular neck.

In dorsal view, the mandibular body is flattened medially, but dorsoventrally convex laterally. The tip of the coronoid process is strongly bent outwards, suggesting that, in life, the adducted mandible was rotated towards the lateral edge of the rostrum. Posterior to the coronoid process, the mandibular foramen is overhung by a moderately developed postcoronoid elevation. The mandibular neck is straight, rather than recurved as in balaenopterids.

Postcrania. In ventral view, the atlas is notably robust. The hypapophysis is reduced to a small protuberance of roughened bone that, judging from its surface texture, may have been weakly fused to the axis. In posterior view, the remainder of the articular surface for the axis, including the well-defined fossa for the odontoid process, is smooth (Fig. 3).

In posterior view, the body of the seventh cervical vertebra is approximately squared. The upper transverse process is relatively slender and oriented anteroventrally. There is no lower transverse process. The posteroventral border of the body is roughed, spongy and somewhat broken, suggesting partial and – presumably – pathological fusion of C7 and T1 (Fig. 3).

In posterior view, the body of the more anterior thoracic vertebra (presumably T3 or T4) is approximately oval (Fig. 6). The transverse process is short and oriented somewhat anteriorly. The body of the more posterior thoracic is far longer anteroposteriorly, and approximately heart-shaped in anterior view. There is no ventral keel. A small anterolateral protuberance approximately halfway up the height of the body presumably represent a semi-facet for the associated rib.

DISCUSSION AND CONCLUSIONS

Identification of the new material as *Tranatocetus*

Tranatocetus maregermanicum closely resembles *T. argillarius* in its (i) overall size, (ii) slender ascending process of the maxilla, (iii) lack of an external occipital crest, (iv) elongate anterior process of the periotic, (v) lack of a lateral tuberosity on the periotic, (vi) low mandibular condyle, (vii) large mandibular fossa, (viii) presence of a posterodorsal platform inside the mandibular fossa, and (ix) deep subcondylar furrow (Fig. 9).

Nevertheless, the original description of *T. argillarius* also lists several features that appear to differentiate the two species. Of these, the most obvious include a smaller angular process of the mandible which seemingly does not extend beyond the level of the mandibular condyle (Gol'din & Steeman 2015, p. 15-12); an even larger mandibular fossa (Gol'din & Steeman 2015, p. 7); a smaller distal exposure of the compound posterior process (Gol'din & Steeman 2015, p. 4); and a somewhat rounded, rather than straight, lateral border of the supraoccipital (Gol'din & Steeman 2015, fig. 1).

Our re-examination of *T. argillarius* suggests that all of these differences can be explained by the poor state of preservation of the holotype (GMUC VP2319). Thus, the angular process of the latter is not preserved, and has been entirely reconstructed in resin, leaving its shape and size in doubt (Roth 1978) (Fig. 10). A morphology similar to that of *T. maregermanicum* therefore cannot be excluded, and perhaps might even be indicted by the similarly pronounced subcondylar furrow in both species.

The size and shape of the mandibular fossa are similarly problematic, as its ventral portion in *T. argillarius* has broken off, and no longer makes direct contact with the remainder of the mandible. During reconstruction, it was fixed into its inferred position with resin, but likely somewhat out of place, and at the wrong angle (Fig. 10). In anterior view, the outer wall of the mandibular fossa curves inwards and becomes markedly thinner towards its ventral border. By contrast, the now juxtaposed ventral portion of the mandible (including the ventral border of the mandibular fossa) is notably less concave and relatively thick, implying that it is not in its original position. Extrapolating the curvature of the outer wall suggests that the cross section of the ramus, and thus also the mandibular fossa, would originally have been smaller, and thus more similar to that of *T. maregermanicum*.

The compound posterior process of *T. argillarius* is extremely poorly preserved on both sides of the skull (Fig. 10). Despite repeated attempts by two of the authors (FGM. and KP), we were unable to trace its outline, thus invalidating it as a diagnostic feature. We note, however, that the space between the external acoustic meatus and the exoccipital is large, and thus consistent with a broadly exposed compound posterior process as seen in *T. maregermanicum*. A large compound posterior process would furthermore match the sizeable paroccipital concavity.

Finally, the supraoccipital is highly fragmentary, which makes its shape difficult to assess. The tip is fixed in place by a large amount of resin, giving rise to an artificially rounded left lateral outline in dorsal view. The right lateral border is comparatively straight, although the supraoccipital shield as a whole still seems somewhat broader and blunter than in *T. maregermanicum*. On the whole, the detailed morphology of this feature likely differs between *T. argillarius* and *T. maregermanicum*, but not as much as the reconstructed skull of the former might suggest.

Based on these observations, we conclude that the features distinguishing the two species of *Tranatocetus* are relatively mild, with the most pronounced differences being attributable to artefacts of preservation. In keeping with the results of our phylogenetic analysis (see below), we therefore reaffirm their placement in the same genus.

Phylogeny and the status of Tranatocetidae

For more than a decade, there has been broad agreement on the basic concept of Cetotheriidae (Bouetel & de Muizon 2006; El Adli et al. 2014; Gol'din & Startsev 2017; Marx & Fordyce 2015; Steeman 2007; Whitmore & Barnes 2008). Nevertheless, the scope of the family has been thrown in doubt by the inclusion of the pygmy right whale, *Caperea marginata* (Fordyce & Marx 2013; Marx & Fordyce 2016; Park et al. 2017), and the proposed grouping of several species usually regarded as cetotheriids into the separate family Tranatocetidae (Gol'din & Steeman 2015). The latter is thought to be more closely related to balaenopterids than to cetotheriids, and comprises the eponymous *Tranatocetus*, as well as *Mesocetus longirostris*, *Mixocetus elysius*, '*Aulocetus latus*', '*Cetotherium*' *megalophysum*, and '*Metopocetus*' *vandelli* (Gol'din & Steeman 2015). Of these, the last three frequently cluster in phylogenetic analyses, and may represent the same genus or even species (El Adli et al. 2014; Gol'din 2018; Marx et al. 2016).

Our phylogenetic analysis contradicts the status of Tranatocetidae as a separate family by recovering *Tranatocetus* deeply nested within Cetotheriidae, as sister to *Metopocetus* (Fig. 11). The same applies to other presumed tranatocetids, including '*Aulocetus*' *latus*, '*Cetotherium*' *megalophysum*, and '*Metopocetus*' *vandelli* (Gol'din & Steeman 2015). The monophyly of Cetotheriidae is primarily supported by the presence of a posteroventral flange on the compound posterior process (char. 184), and the parabolic outline of the postglenoid process (char. 118, in posterior view). Additional characters shared by all cetotheriids except *Tiucetus* and *Joumocetus* include ascending processes of the maxillae that directly contact the nasals (char. 67, reversed in cetotheriines), parietals that extend no further forward than the level of the postorbital process (char. 81), a distal surface of the compound posterior process that is firmly integrated into the lateral skull wall (char. 188), a squared anterior border of the tympanic bulla (char. 191), deep transverse creases on the dorsal surface of the involucrum (char. 207), and a mandibular body that increases in height towards the symphyseal area (char. 222, in lateral view).

Several features were previously noted as distinguishing tranatocetids from cetotheriids, including a smaller distal exposure of the compound posterior process, a narrower anterior portion of the tympanic bulla, a small angular process of the mandible, a low mandibular condyle, and a shallow glenoid fossa (Gol'din & Steeman 2015).

The exposure of the compound posterior process is variable among cetotheriids, with the process being broadly exposed in herpetocetines, cetotheriines (sensu Gol'din & Startsev 2017), *Herentalia*, *Metopocetus* and *Piscobalaena*, but less so in *Joumocetus* and *Tiucetus*. This range presumably is the result of a trend, with the basalmost taxa also having the smallest exposures (Kimura & Hasegawa 2010; Marx et al. 2017). Tranatocetids fit different parts of this spectrum, with the exposed surface of *Tranatocetus* being comparable to that of *Herentalia* and *Metopocetus*, and far larger than in '*Aulocetus*' *latus*, '*Cetotherium*' *megalophysum* and '*Metopocetus*' *vandelli*. All tranatocetids furthermore share with cetotheriids a common structure of the compound posterior process, with the latter being expanded distally, and bearing a posteroventral flange which partially floors the facial sulcus (Figs 7, 12) (Marx et al. 2016; Marx & Fordyce 2016). Tranatocetids therefore do not systematically differ in the morphology of their compound posterior process, but form part of morphological continuum encompassing all of Cetotheriidae.

Like the compound posterior process, the shape of the tympanic bulla is variable among cetotheriids. In ventral view, the anterior portion of the bulla is equal to or wider than the posterior half in *Herpetocetus* and cetotheriines, slightly narrower in *Ciuciulea*, and notably narrower in *Metopocetus* and *Piscobalaena* (Fig. 12). In most cetotheriids – in particular, cetotheriines and *Piscobalaena* – the anterior border of the tympanic bulla is furthermore notably squared. Tranatocetids generally conform to the narrow morphotype, including the squared anterior border, and thus tend to resemble *Piscobalaena*. (Fig. 12). We agree that narrowing of the anterior bulla may be a derived state setting apart certain species in the broader context of Cetotheriidae. Nevertheless, as shown by the striking resemblance of '*C.*' *megalophysum* and *Piscobalaena* (Fig. 12), there is no clear division between this morphology and that of several undoubted cetotheriids.

The angular process of the mandible tends to be enlarged in Cetotheriidae, either dorsoventrally as in cetotheriines (Gol'din et al. 2014; Gol'din 2018), or anteroposteriorly as in *Piscobalaena* and herpetocetines (Bouetel & de Muizon 2006; El Adli et al. 2014). In the latter two, the process notably projects beyond the level of the mandibular condyle, and bears a well-developed fossa for the medial pterygoid muscle. Our new observations show that *Tranatocetus* precisely fits this elongate morphotype (Fig. 8), nesting it deep within Cetotheriidae. The mandibular morphology of other 'tranatocetids' is poorly known, with no lower jaws having been described for '*A.*' *latus*, '*C.*' *megalophysum* and '*M.*' *vandelli*.

A comparatively small angular process, as previously suggested for tranatocetids (Gol'din & Steeman 2015), appears to be the plesiomorphic state, based on its occurrence in both balaenopterids and a variety of Miocene non-cetotheriids (Kellogg 1934; Kellogg 1968a; Steeman 2009; Tanaka et al. 2018a). In light of this observation, we question the usefulness of this feature as a distinguishing characteristic of tranatocetids, and predict that basal cetotheriids, such as *Joumocetus* and *Tiucetus*, may ultimately be revealed to have a markedly smaller angular process than other members of the family.

Like a small angular process, a low mandibular condyle appears to be a plesiomorphic feature characterising both balaenopterids and a broad range of Miocene non-cetotheriid mysticetes (Kellogg 1934; Kellogg 1968a; Kellogg 1968b; Kimura 2002; Tanaka et al. 2018a). By contrast, the condyle of cetotheriids tends to be somewhat elevated above the mandibular neck. The position and orientation of the condyle in turn correlates with that of the glenoid fossa of the squamosal, with the latter reportedly being relatively shallow in cetotheriids (Gol'din et al. 2014; Gol'din & Steeman 2015).

Tranatocetus has a posteriorly oriented, non-elevated condyle, and – in this regard – shows a relatively primitive morphology of the craniomandibular joint (Figs 8, 9). This anatomy could plausibly be plesiomorphic but, considering the otherwise clearly cetotheriid shape of the ramus, might also represent a secondary feature, perhaps associated with large body size. The anatomy of '*A.*' *latus*, '*C.*' *megalophysum* and '*M.*' *vandelli* remains unknown. As with a small angular process, we predict that a low mandibular condyle also primitively occurred in some basal cetotheriids, and thus is of limited value in distinguishing the latter from tranatocetids.

Overall, it thus appears as though the evidence supporting a separation of Cetotheriidae and Tranatocetidae is relatively weak. By contrast, our new observations on *Tranatocetus* reveal a marked resemblance of this genus with several undoubted cetotheriids, borne out by the results of our phylogenetic analysis. These results cast doubt on the status of Tranatocetidae as a separate family, and instead imply the existence of a single, extended family Cetotheriidae, including *Tiucetus* as its basalmost form.

Implications for cetotheriid palaeobiology

At an estimated body length of 7.7 m (based on Lambert et al. 2010) to 8.7 m (based on Pyenson & Sponberg 2011), *Tranatocetus maregermanicum* is the largest formally described cetotheriid. In stark contrast, most of the other members of the family do not exceed 5 m in length, and thus are relatively small compared to other mysticetes (Bouetel & de Muizon 2006; El Adli et al. 2014; Gol'din & Startsev 2017; Gol'din 2018; Slater et al. 2017). There are, however, notable exceptions, including *Herentalia nigra*, '*Cetotherium*' *megalophysum*, an as yet unnamed species from Peru, and a fragmentary skeleton from northern Belgium (Bisconti 2015; Bosselaers et al. 2004; Collareta et al. 2015; Slater et al. 2017).

In general, larger cetotheriids appear to cluster in the early Late Miocene, whereas smaller forms – in particular, herpetocetines, and *Piscobalaena* – dominate during the latest Miocene and Pliocene (Bouetel & de Muizon 2006; El Adli et al. 2014; Tanaka et al. 2018b; Tanaka & Watanabe 2018; Whitmore & Barnes 2008). Larger size plausibly correlated with a different ecological niche, with *Tranatocetus* perhaps being more pelagic than other cetotheriids, or targeting free-swimming schooling fish instead of benthos. The same may have applied to other large cetotheriids (Collareta et al. 2015), and possibly suggests a Late Miocene shift towards a different diet, habitat or feeding strategy.

The reasons behind this shift, ~~in~~ indeed it occurred, remain obscure, but it seems noteworthy that it coincided with the initial diversification of rorquals. In the Pisco Formation of Peru, for example, rorquals became locally abundant, and represented by two to three different species (Di Celma et al. 2017), at the same time as cetotheriids declined in number and size (Bianucci et al. 2016a; Bianucci et al. 2016b). We suggest that this phenomenon might be explained by niche partitioning between small, suction feeding and possibly benthic/neritic cetotheriids on the one hand (El Adli et al. 2014; Gol'din et al. 2014), and large, lunge-feeding, pelagic rorquals on the other. Cetotheriids subsequently occupied the 'small (benthic) filter feeder' niche for the remainder of the Pliocene, but then largely disappeared, along with small balaenids and most small rorquals, with the onset of Northern Hemisphere glaciation around 3 Ma (Marx & Fordyce 2015; Slater et al. 2017).

ACKNOWLEDGEMENTS

We thank Remie Bakker and Tone Skelton for hosting us, and their help in mounting the specimen; Bram Langeveld and Henry van der Es for their assistance at NMR; Mette Steeman for the warm reception at Gram; Pavel Gol'din for helpful discussions on cetotheriid systematics; Carl Buell for providing illustrative drawings of living and fossil cetaceans; and the staff of all of the institutions involved for access to material and help during our visits.

REFERENCES

Bianucci G, Di Celma C, Collareta A, Landini W, Post K, Tinelli C, de Muizon C, Bosio G, Gariboldi K, Gioncada A, Malinverno E, Cantalamessa G, Altamirano-Sierra A, Salas-Gismondi R, Urbina M, and Lambert O. 2016a. Fossil marine vertebrates of Cerro Los Quesos: distribution of cetaceans, seals, crocodiles, seabirds, sharks, and bony fish in a late Miocene locality of the Pisco Basin, Peru. *Journal of Maps* 12:1037-1046. 10.1080/17445647.2015.1115785

Bianucci G, Di Celma C, Landini W, Post K, Tinelli C, de Muizon C, Gariboldi K, Malinverno E, Cantalamessa G, Gioncada A, Collareta A, Gismondi R-S, Varas-Malca R, Urbina M, and Lambert O. 2016b. Distribution of fossil marine vertebrates in Cerro Colorado, the type locality of the giant raptorial sperm whale *Livyatan melvillei* (Miocene, Pisco Formation, Peru). *Journal of Maps* 12:543-557. 10.1080/17445647.2015.1048315

Bisconti M. 2015. Anatomy of a new cetotheriid genus and species from the Miocene of Herentals, Belgium, and the phylogenetic and palaeobiogeographical relationships of Cetotheriidae s.s. (Mammalia, Cetacea, Mysticeti). *Journal of Systematic Palaeontology* 13:377-395. 10.1080/14772019.2014.890136

Boessenecker RW. 2011. Herpetocetine (Cetacea: Mysticeti) dentaries from the Upper Miocene Santa Margarita Sandstone of Central California. *Paleobios* 30:1-12.

Bosselaers M, Herman J, Hoedemakers K, Lambert O, Marquet R, and Wouters K. 2004. Geology and palaeontology of a temporary exposure of the Late Miocene Deurne Sand Member in Antwerpen (N. Belgium). *Geologica Belgica* 7:27-39.

Bouetel V, and de Muizon C. 2006. The anatomy and relationships of *Piscobalaena nana* (Cetacea, Mysticeti), a Cetotheriidae s.s. from the early Pliocene of Peru. *Geodiversitas* 28:319-395.

Collareta A, Landini W, Lambert O, Post K, Tinelli C, Di Celma C, Panetta D, Tripodi M, Salvadori P, Caramella D, Marchi D, Urbina M, and Bianucci G. 2015. Piscivory in a Miocene Cetotheriidae of Peru: first record of fossilized stomach content for an extinct baleen-bearing whale. *The Science of Nature* 102:1-12. 10.1007/s00114-015-1319-y

de Verteuil L, and Norris G. 1996. Miocene dinoflagellate stratigraphy and systematics of Maryland and Virginia. *Micropaleontology* 42 (Suppl.):1-172.

Di Celma C, Malinverno E, Bosio G, Collareta A, Gariboldi K, Gioncada A, Molli G, Basso D, Varas-Malca R, Pierantoni PP, Villa IM, Lambert O, Landini W, Sarti G, Cantalamessa G, Urbina M, and Bianucci G. 2017. Sequence stratigraphy and paleontology of the Upper Miocene Pisco Formation along the western side of the lower Ica Valley (Ica Desert, Peru). *Rivista Italiana di Paleontologia e Stratigrafia* 123:255-274.

Dybkjær K, and Piasecki S. 2010. Neogene dinocyst zonation for the eastern North Sea Basin, Denmark. *Review of Palaeobotany and Palynology* 161:1-29. http://dx.doi.org/10.1016/j.revpalbo.2010.02.005

El Adli JJ, Deméré TA, and Boessenecker RW. 2014. *Herpetocetus morrowi* (Cetacea: Mysticeti), a new species of diminutive baleen whale from the Upper Pliocene (Piacenzian) of California, USA, with observations on the evolution and relationships of the Cetotheriidae. *Zoological Journal of the Linnean Society* 170:400-466. 10.1111/zoj.12108

Fordyce RE, and Marx FG. 2013. The pygmy right whale *Caperea marginata*: the last of the cetotheres. *Proceedings of the Royal Society B* 280:20122645. 10.1098/rspb.2012.2645

Fordyce RE, and Marx FG. 2018. Gigantism precedes filter feeding in baleen whale evolution. *Current Biology* 28:1670-1676.e1672. 10.1016/j.cub.2018.04.027

Gol'din P, Startsev D, and Krakhmalnaya T. 2014. The anatomy of the Late Miocene baleen whale *Cetotherium riabinini* from Ukraine. *Acta Palaeontologica Polonica* 59:795-814. http://dx.doi.org/10.4202/app.2012.0107

Gol'din P, and Steeman ME. 2015. From problem taxa to problem solver: a new Miocene family, Tranatocetidae, brings perspective on baleen whale evolution. *PLOS ONE* 10:e0135500. 10.1371/journal.pone.0135500

Gol'din P, and Startsev D. 2017. A systematic review of cetothere baleen whales (Cetacea, Cetotheriidae) from the Late Miocene of Crimea and Caucasus, with a new genus. *Papers in Palaeontology* 3:49-68. 10.1002/spp2.1066

Gol'din P. 2018. New Paratethyan dwarf baleen whales mark the origin of cetotheres. *PeerJ* 6:e5800. 10.7717/peerj.5800

Kellogg R. 1929. A new cetothere from southern California. *University of California Publications in Geological Sciences* 18:449-457.

Kellogg R. 1934. The Patagonian fossil whalebone whale, *Cetotherium moreni* (Lydekker). *Carnegie Institution of Washington Publication* 447:64–81.

Kellogg R. 1968a. Fossil marine mammals from the Miocene Calvert Formation of Maryland and Virginia, part 8: supplement to the description of *Parietobalaena palmeri United States National Museum Bulletin* 247:175-197.

Kellogg R. 1968b. Fossil marine mammals from the Miocene Calvert Formation of Maryland and Virginia, part 6: a hitherto unrecognized Calvert cetothere. *United States National Museum Bulletin* 247:133-161.

Kimura T. 2002. Feeding strategy of an Early Miocene cetothere from the Toyama and Akeyo Formations, central Japan. *Paleontological Research* 6:179-189.

Kimura T, and Hasegawa Y. 2010. A new baleen whale (Mysticeti: Cetotheriidae) from the earliest late Miocene of Japan and a reconsideration of the phylogeny of cetotheres. *Journal of Vertebrate Paleontology* 30:577-591. 10.1080/02724631003621912

Lambert O, Bianucci G, Post K, de Muizon C, Salas-Gismondi R, Urbina M, and Reumer J. 2010. The giant bite of a new raptorial sperm whale from the Miocene epoch of Peru. *Nature* 466:105-108. 10.1038/nature09067

Louwye S, and de Schepper S. 2010. The Miocene–Pliocene hiatus in the southern North Sea Basin (northern Belgium) revealed by dinoflagellate cysts. *Geological Magazine* 147:760-776. doi:10.1017/S0016756810000191

Marx FG, and Fordyce RE. 2015. Baleen boom and bust: a synthesis of mysticete phylogeny, diversity and disparity. *Royal Society Open Science* 2:140434.

Marx FG, Bosselaers MEJ, and Louwye S. 2016. A new species of *Metopocetus* (Cetacea, Mysticeti, Cetotheriidae) from the Late Miocene of the Netherlands. *PeerJ* 4:e1572. 10.7717/peerj.1572

Marx FG, and Fordyce RE. 2016. A link no longer missing: new evidence for the cetotheriid affinities of *Caperea*. *PLOS ONE* 11:e0164059. 10.1371/journal.pone.0164059

Marx FG, Lambert O, and de Muizon C. 2017. A new Miocene baleen whale from Peru deciphers the dawn of cetotheriids. *Royal Society Open Science* 4:170560. 10.1098/rsos.170560

Mead JG, and Fordyce RE. 2009. The therian skull: a lexicon with emphasis on the odontocetes. *Smithsonian Contributions to Zoology* 627:1-248.

Miller MA, Pfeiffer W, and Schwartz T. 2010. Creating the CIPRES Science Gateway for inference of large phylogenetic trees. Proceedings of the Gateway Computing Environments Workshop (GCE), 14 Nov 2010. New Orleans. p 1-8.

Munsterman DK, and Brinkhuis H. 2004. A southern North Sea Miocene dinoflagellate cyst zonation. *Geologie en Mijnbouw* 83:267-285.

Ogg JG, Ogg GM, and Gradstein FM. 2016. *A Concise Geologic Time Scale 2016*. Ed. Amsterdam: Elsevier.

Park T, Marx FG, Fitzgerald EMG, and Evans AR. 2017. The cochlea of the enigmatic pygmy right whale *Caperea marginata* informs mysticete phylogeny. *Journal of Morphology* 278:801-809. 10.1002/jmor.20674

Post K, and Reumer JWF. 2016. History and future of paleontological surveys in the Westerschelde Estuary (Province of Zeeland, the Netherlands). *Deinsea*.

Pyenson ND, and Sponberg SN. 2011. Reconstructing body size in extinct crown Cetacea (Neoceti) using allometry, phylogenetic methods and tests from the fossil record. *Journal of Mammalian Evolution* 18:269-288. 10.1007/s10914-011-9170-1

Roth F. 1978. *Mesocetus argillarius* sp.n. (Cetacea, Mysticeti) from Upper Miocene of Denmark, with remarks on the lower jaw and the echolocation system in whale phylogeny. *Zoologica Scripta* 7:63-79. 10.1111/j.1463-6409.1978.tb00589.x

Saita N, Komukai S, and Oishi M. 2011. A small fossil whale from the Tatsunokuchi Formation (uppermost Miocene to Lower Pliocene) of Sendai City, Northeast Japan: Its occurrence, age and paleontological significance. *Bulletin of the Tohoku University Museum* 10:135–146.

Slater GJ, Goldbogen JA, and Pyenson ND. 2017. Independent evolution of baleen whale gigantism linked to Plio-Pleistocene ocean dynamics. *Proceedings of the Royal Society B: Biological Sciences* 284:20170546. 10.1098/rspb.2017.0546

Steeman ME. 2007. Cladistic analysis and a revised classification of fossil and recent mysticetes. *Zoological Journal of the Linnean Society* 150:875-894.

Steeman ME. 2009. A new baleen whale from the Late Miocene of Denmark and early mysticete hearing. *Palaeontology* 52:1169-1190. 10.1111/j.1475-4983.2009.00893.x

Tanaka Y, Ando T, and Sawamura H. 2018a. A new species of Middle Miocene baleen whale from the Nupinai Group, Hikatagawa Formation of Hokkaido, Japan. *PeerJ* 6:e4934. 10.7717/peerj.4934

Tanaka Y, Furusawa H, and Barnes LG. 2018b. Fossil herpetocetine baleen whales (Cetacea, Mysticeti, Cetotheriidae) from the Lower Pliocene Horokaoshirarika Formation at Numata, Hokkaido, northern Japan. *Paleontological Research* 22:295-306. 10.2517/2017PR025

Tanaka Y, and Watanabe M. 2018. Geologically old and ontogenetically young *Herpetocetus* sp. from the late Miocene of Hokkaido, Japan. *Journal of Vertebrate Paleontology*:1-11. 10.1080/02724634.2018.1478842

Whitmore FC, Jr, and Barnes LG. 2008. The Herpetocetinae, a new subfamily of extinct baleen whales (Mammalia, Cetacea, Cetotheriidae). *Virginia Museum of Natural History Special Publication* 14:141-180.

Williams GL, Brinkhuis H, Pearce MA, Fensome RA, and Weegink JW. 2004. Southern Ocean and global dinoflagellate cyst events compared: index events for the Late Cretaceous–Neogene. *Proceedings of the Ocean Drilling Program Scientific Results* 189:1–98.

Williams GL, Fensome RA, and MacRae RA. 2017. Lentin and Williams index of fossil dinoflagellates. *AASP Contributions Series* 48:1-1097.

Figure captions

Figure 1. Type locality (A) and horizon (B) of *Tranatocetus maregermanicum*. Curly bracket in (B) marks the type horizon, as judged from the dinoflagellate fauna associated with the whale fossils. (B) modified from Ogg et al. (2016). Drawing of cetotheriid by Carl Buell.

Figure 2. Holotype cranium of *Tranatocetus maregermanicum* (NMR9991-16680) in dorsal view.

Figure 3. Paratype cranium of *Tranatocetus maregermanicum* (NMR9991-16681) in (A) ventral and (B) posterior view.

Figure 4. Holotype cranium of *Tranatocetus maregermanicum* (NMR9991-16680) in oblique right anterolateral view.

Figure 5. Holotype cranium of *Tranatocetus maregermanicum* (NMR9991-16680) in (A) lateral and (B) anterior view.

Figure 6. Holotype cranium of *Tranatocetus maregermanicum* (NMR9991-16680) in ventral view.

Figure 7. Auditory anatomy of *Tranatocetus maregermanicum*. (A) Auditory region of the holotype cranium (NMR9991-16680) in oblique right posterolateral view. (B) Periotic of the paratype (NMR9991-16681) in ventral view.

Figure 8. Holotype mandible of *Tranatocetus maregermanicum* (NMR9991-16680) in (A) lateral and (B) medial view.

Figure 9. Comparison of the mandibular ramus of (A, C) *Tranatocetus maregermanicum* (NMR9991-16680, holotype) and (B, D) *Tranatocetus argillarius* (GMUC VP2319, holotype) in (A, B) medial, (C) lateral and (D) posterior view.

Figure 10. Damage to the mandible and auditory region of *Tranatocetus argillarius* (GMUC VP2319, holotype). Mandible in (A) anterior, (B) medial and (C) lateral view. (D) Auditory region in oblique right posterolateral view.

Figure 11. Results of the total evidence phylogenetic analysis, showing the nesting of tranatocetids, including *Tranatocetus* itself, inside Cetotheriidae.

Figure 12. Comparison of the auditory regions of (A, C) the presumed tranatocetid '*Cetotherium*' *megalophysum* (USNM 10593, holotype) and (B, D) the cetotheriid *Piscobalaena nana* (MNHN SAS 1616). (A, B) Auditory region in ventral view. (C, D) Compound posterior process in (C) ventrolateral and (D) oblique posterolateral view.

Figure 1(on next page)

Type locality (A) and horizon (B) of *Tranatocetus maregermanicum*.

Curly bracket in (B) marks the type horizon, as judged from the dinoflagellate fauna associated with the whale fossils. (B) modified from Ogg et al. (2016). Drawing of cetotheriid by Carl Buell.

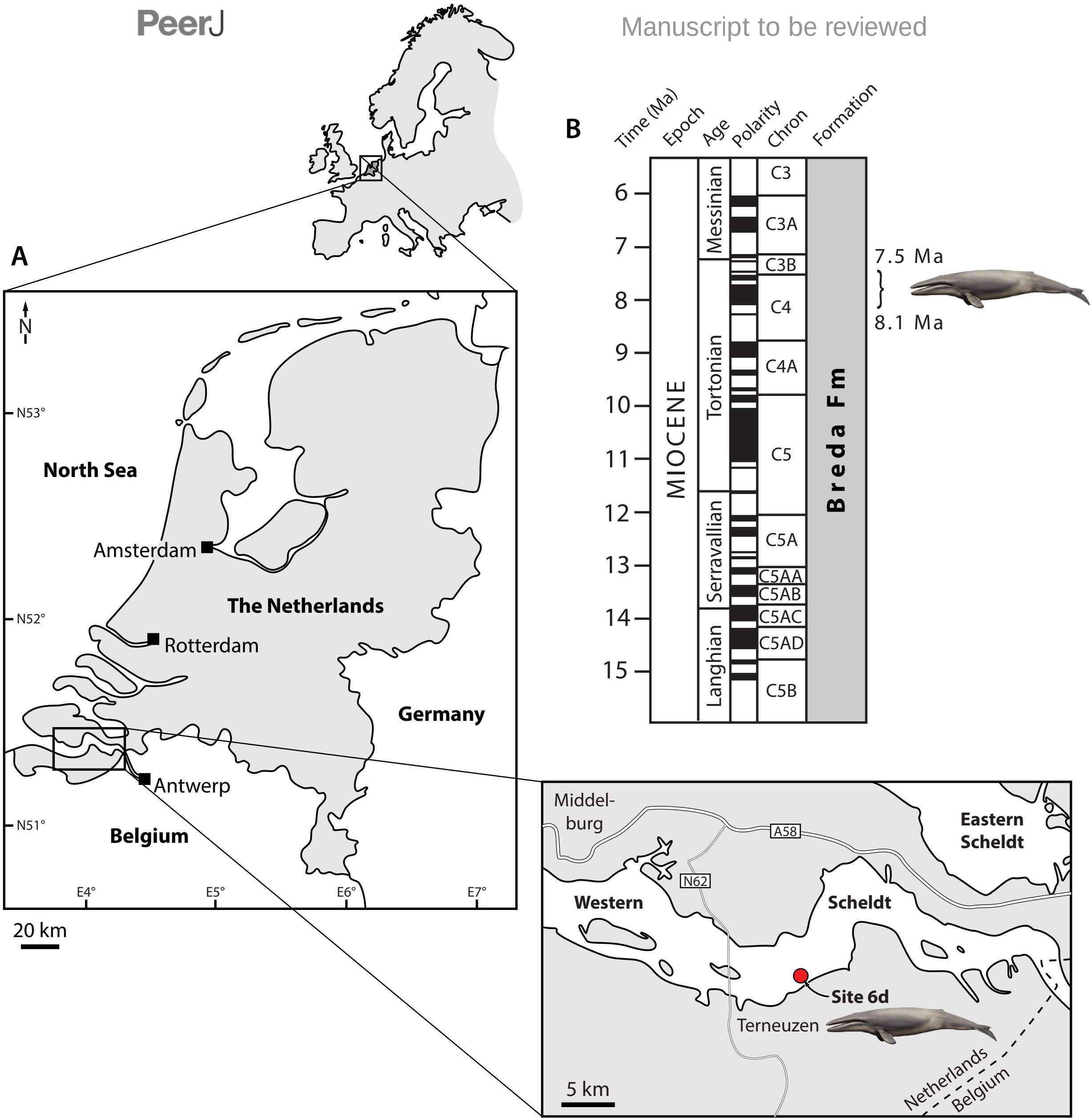
A
N
N53°
N52°
N51°
E4°
E5°
E6°
E7°
North Sea
Amsterdam
The Netherlands
Rotterdam
Germany
Antwerp
Belgium
20 km
B
Time (Ma)
Epoch
Age
Polarity
Chron
Formation
6
7
8
9
10
11
12
13
14
15
MIOCENE
Messinian
Tortonian
Serravallian
Langhian
C3
C3A
C3B
C4
C4A
C5
C5A
C5AA
C5AB
C5AC
C5AD
C5B
Breda Fm
7.5 Ma
8.1 Ma
Middel-
burg
A58
N62
Eastern
Scheldt
Western
Scheldt
Site 6d
Terneuzen
5 km
Netherlands
Belgium

Figure 2 (on next page)

Holotype cranium of *Tranatocetus maregermanicum* (NMR9991-16680) in dorsal view.

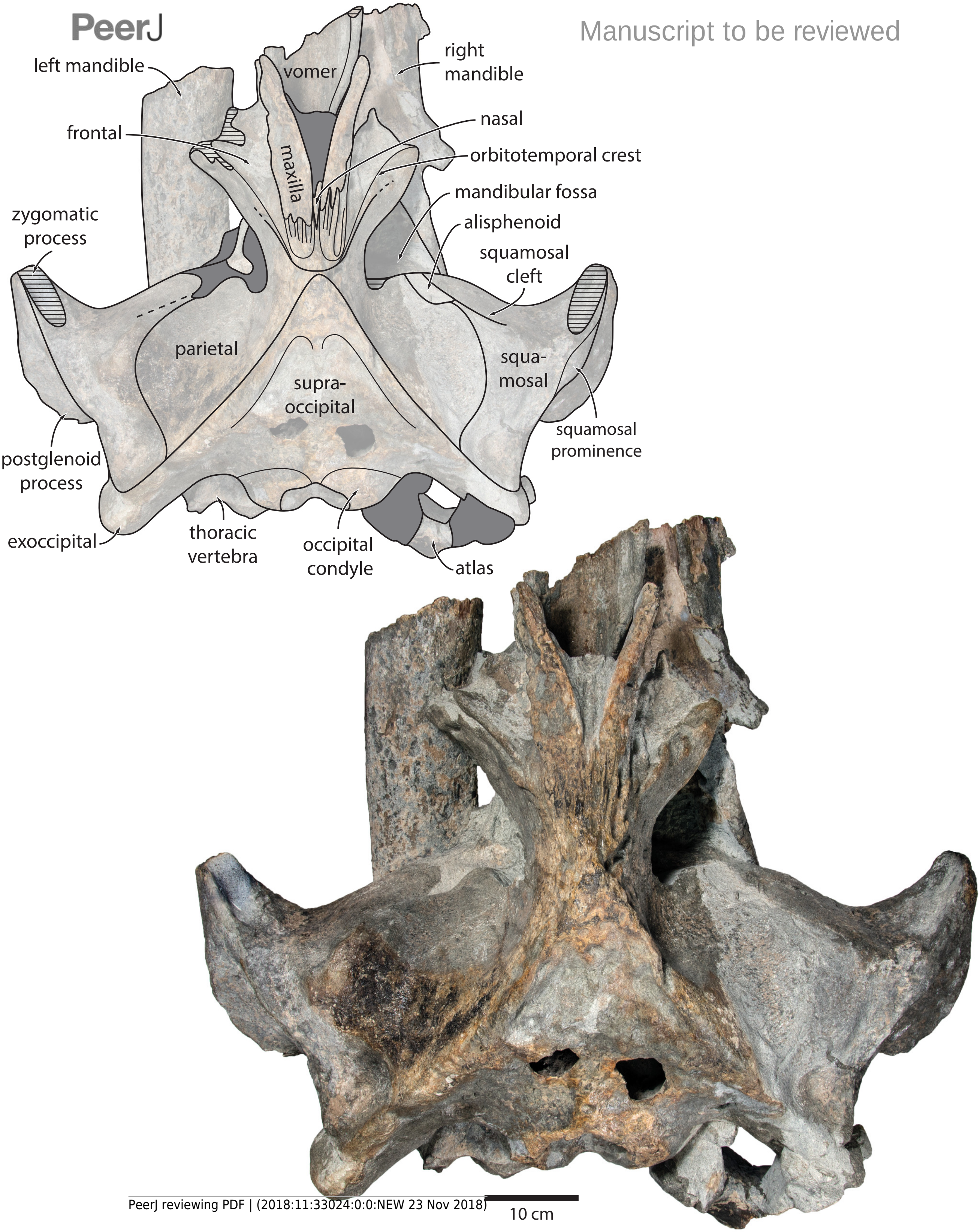
left mandible
vomer
right mandible
frontal
nasal
maxilla
orbitotemporal crest
mandibular fossa
zygomatic process
alisphenoid
squamosal cleft
parietal
squa-
mosal
supra-
occipital
squamosal prominence
postglenoid process
exoccipital
thoracic vertebra
occipital condyle
atlas
10 cm

Figure 3 (on next page)

Paratype cranium of *Tranatocetus maregermanicum* (NMR9991-16681) in (A) ventral and (B) posterior view.

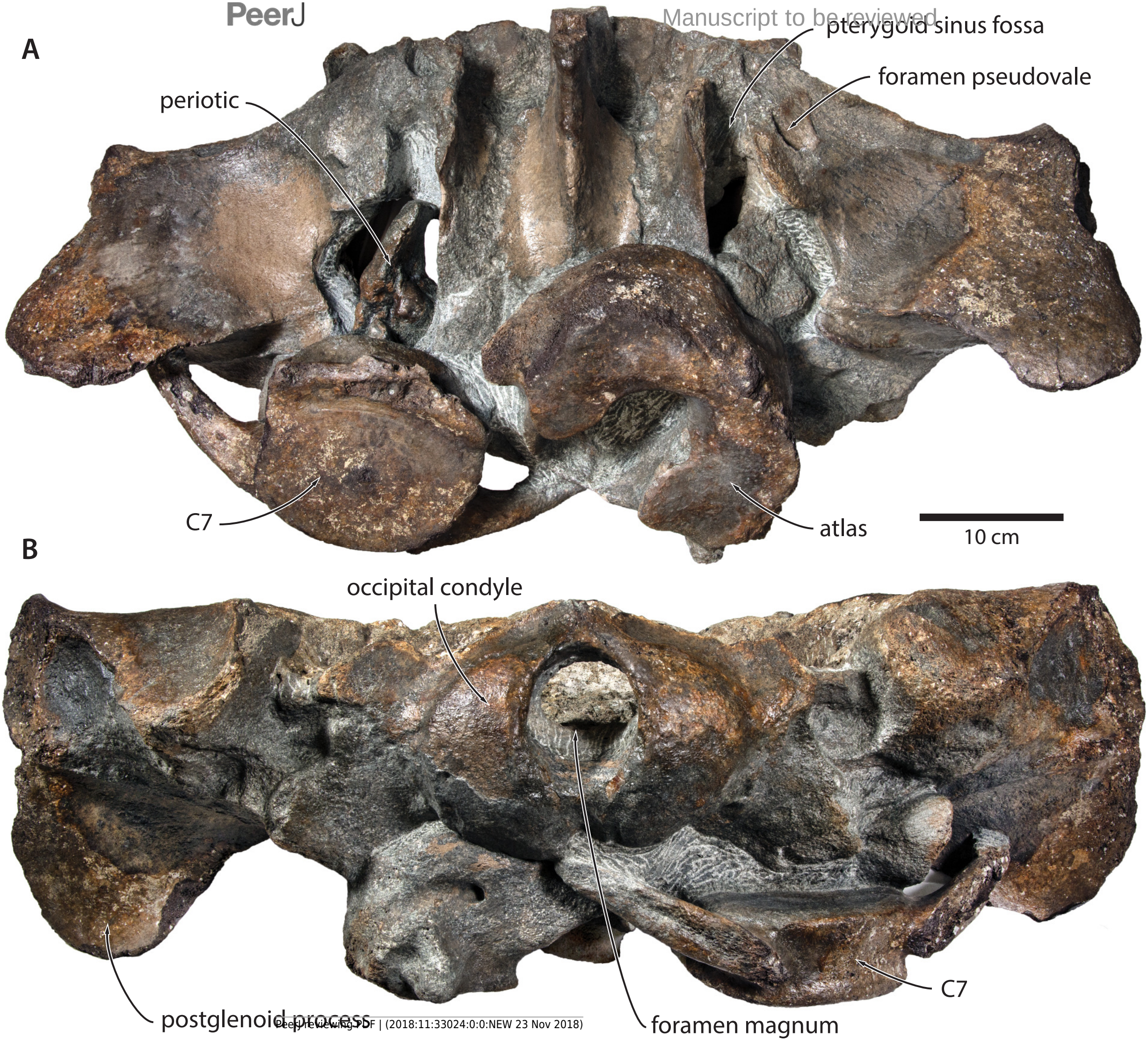
A
pterygoid sinus fossa
foramen pseudovale
periotic
C7
atlas
10 cm
B
occipital condyle
postglenoid process
foramen magnum
C7

Figure 4(on next page)

Holotype cranium of *Tranatocetus maregermanicum* (NMR9991-16680) in oblique right anterolateral view.

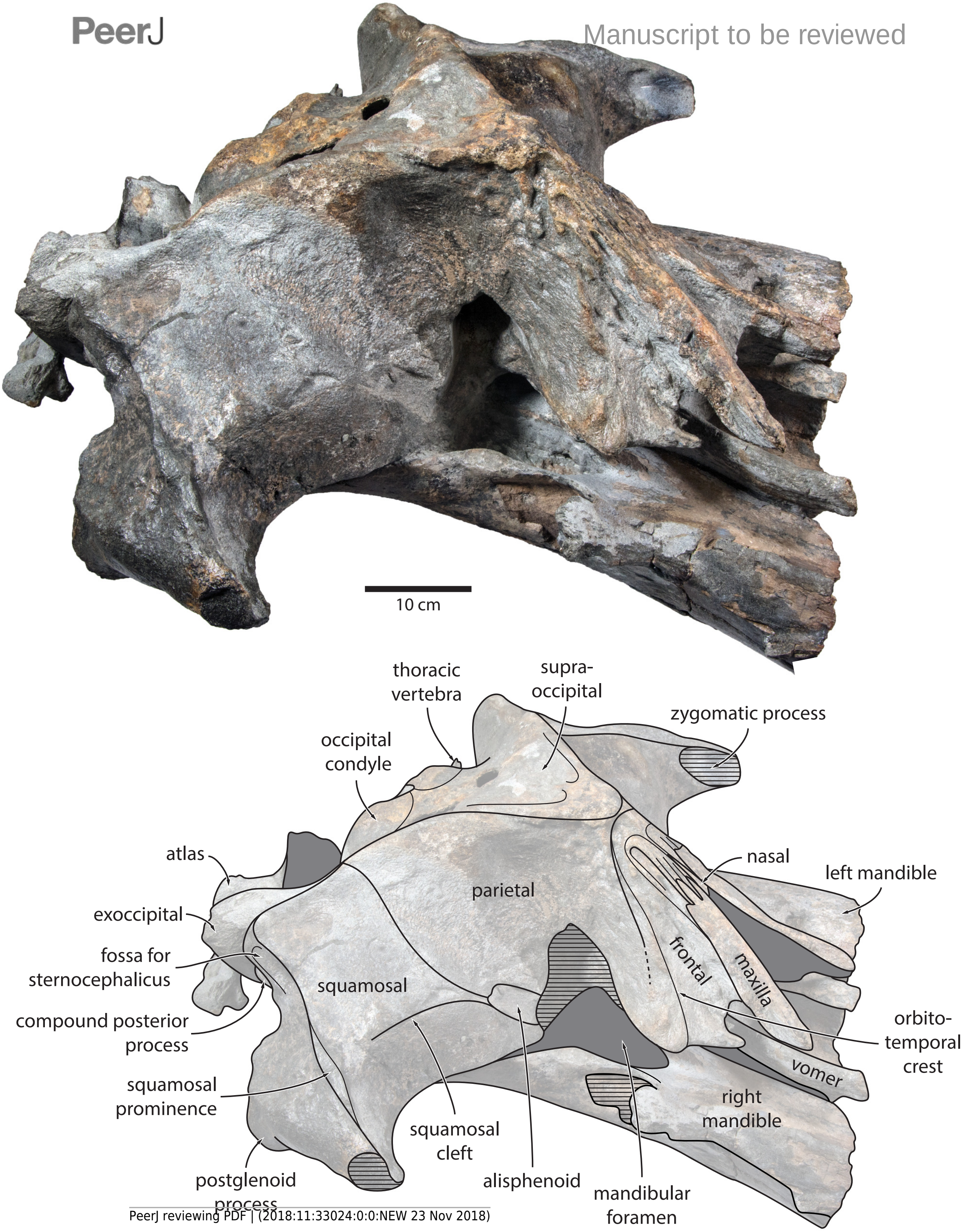
10 cm
thoracic vertebra
supra-occipital
zygomatic process
occipital condyle
atlas
nasal
left mandible
parietal
exoccipital
fossa for sternocephalicus
frontal
maxilla
squamosal
compound posterior process
orbito-temporal crest
vomer
squamosal prominence
right mandible
squamosal cleft
postglenoid process
alisphenoid
mandibular foramen

Figure 5(on next page)

Holotype cranium of *Tranatocetus maregermanicum* (NMR9991-16680) in (A) lateral and (B) anterior view.

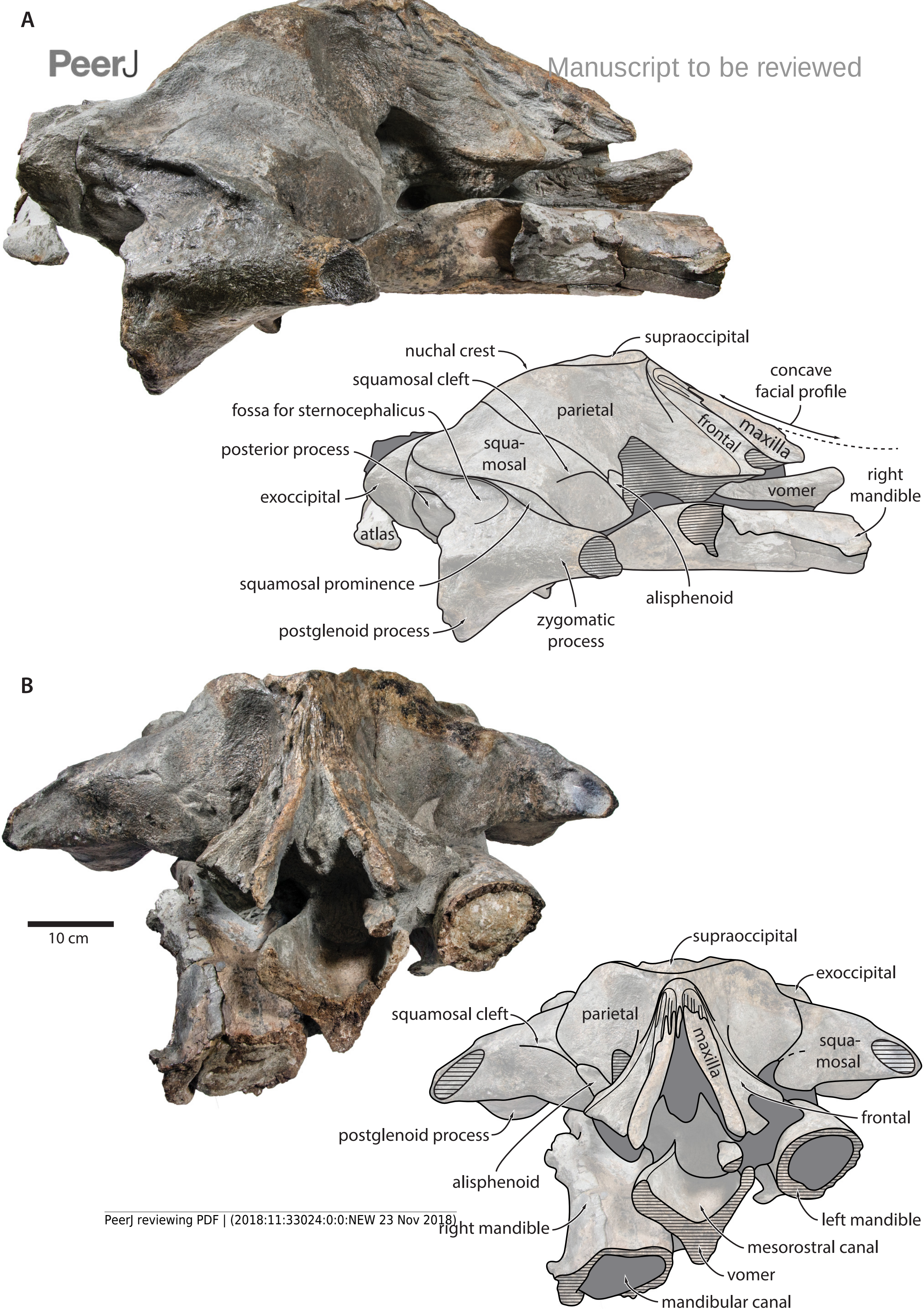
A
nuchal crest
supraoccipital
squamosal cleft
concave
facial profile
fossa for sternocephalicus
parietal
posterior process
squa-
mosal
frontal
maxilla
exoccipital
vomer
right
mandible
atlas
squamosal prominence
alisphenoid
postglenoid process
zygomatic
process
B
10 cm
supraoccipital
exoccipital
squamosal cleft
parietal
maxilla
squa-
mosal
frontal
postglenoid process
alisphenoid
left mandible
right mandible
mesorostral canal
vomer
mandibular canal

Figure 6 (on next page)

Holotype cranium of *Tranatocetus maregermanicum* (NMR9991-16680) in ventral view.

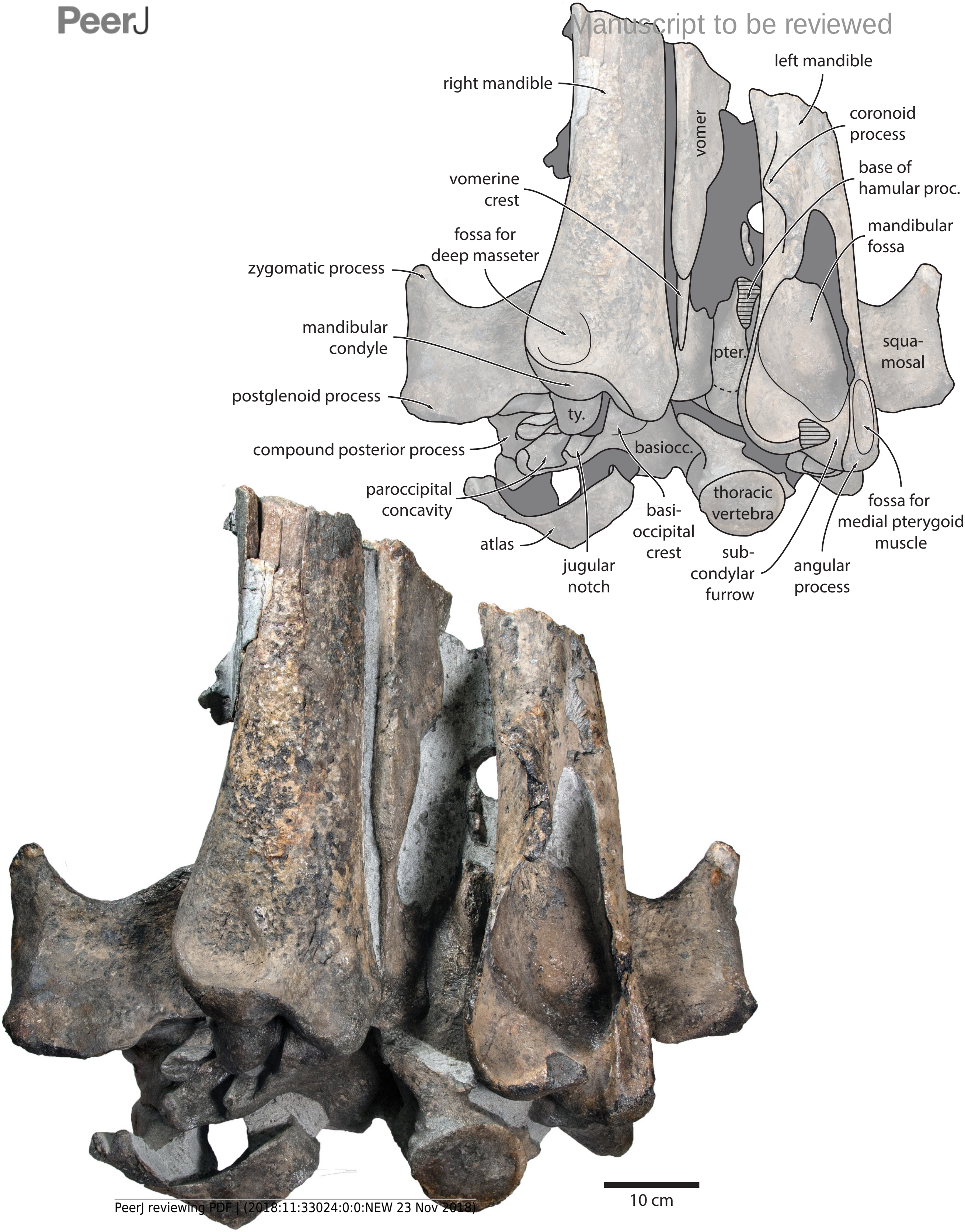
right mandible
vomer
left mandible
coronoid
process
vomerine
crest
base of
hamular proc.
fossa for
deep masseter
mandibular
fossa
zygomatic process
mandibular
condyle
pter.
squa-
mosal
postglenoid process
ty.
compound posterior process
basiocc.
paroccipital
concavity
thoracic
vertebra
atlas
basi-
occipital
crest
jugular
notch
sub-
condylar
furrow
angular
process
fossa for
medial pterygoid
muscle
10 cm

Figure 7 (on next page)

Auditory anatomy of *Tranatocetus maregermanicum.*

(A) Auditory region of the holotype cranium (NMR9991-16680) in oblique right posterolateral view. (B) Periotic of the paratype (NMR9991-16681) in ventral view.

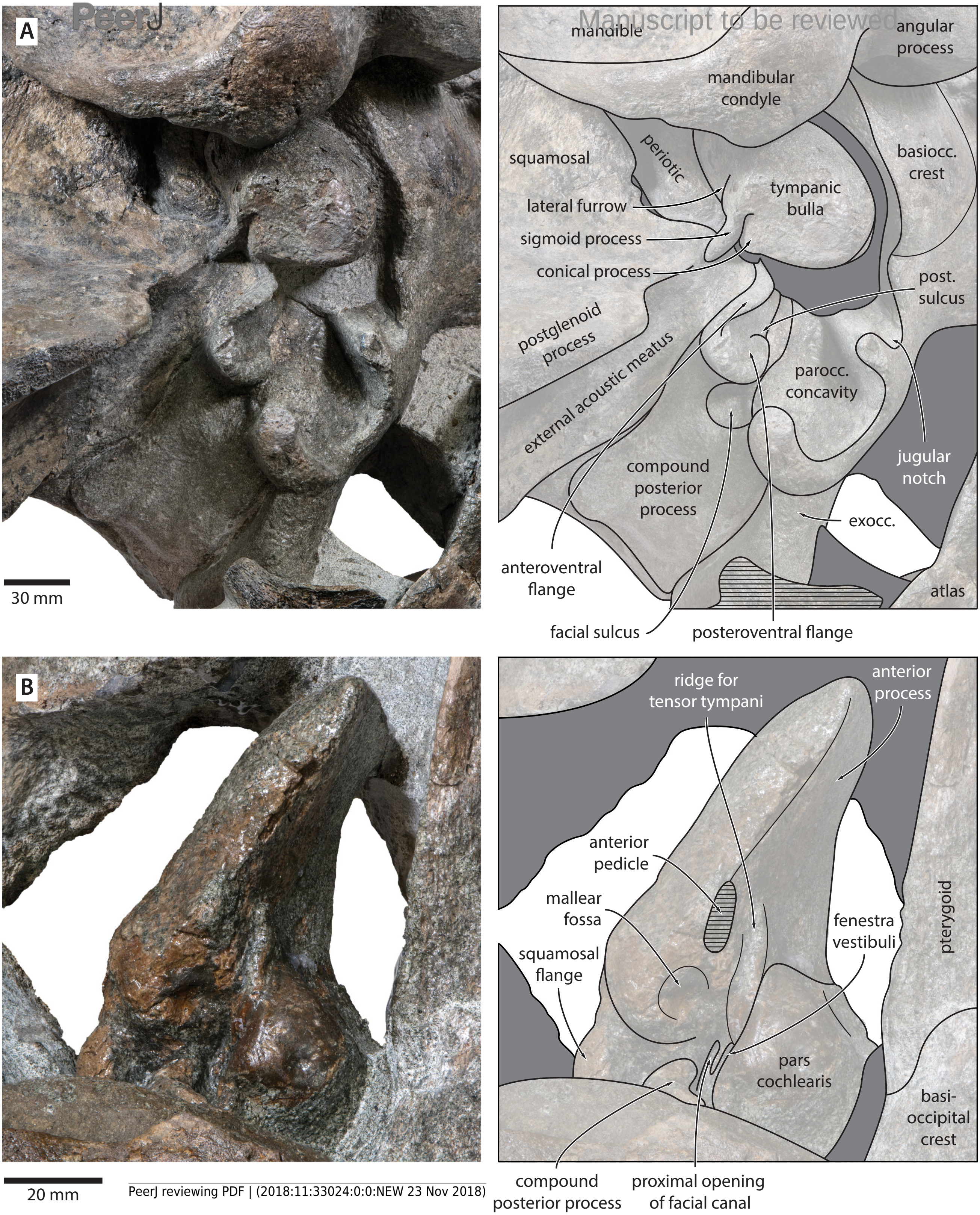
A
30 mm
mandible
angular process
mandibular condyle
squamosal
periotic
basiocc. crest
tympanic bulla
lateral furrow
sigmoid process
conical process
post. sulcus
postglenoid process
external acoustic meatus
parocc. concavity
jugular notch
compound posterior process
exocc.
anteroventral flange
atlas
facial sulcus
posteroventral flange
B
20 mm
ridge for tensor tympani
anterior process
anterior pedicle
mallear fossa
fenestra vestibuli
pterygoid
squamosal flange
pars cochlearis
basi- occipital crest
compound posterior process
proximal opening of facial canal

Figure 8 (on next page)

Holotype mandible of *Tranatocetus maregermanicum* (NMR9991-16680) in (A) lateral and (B) medial view.

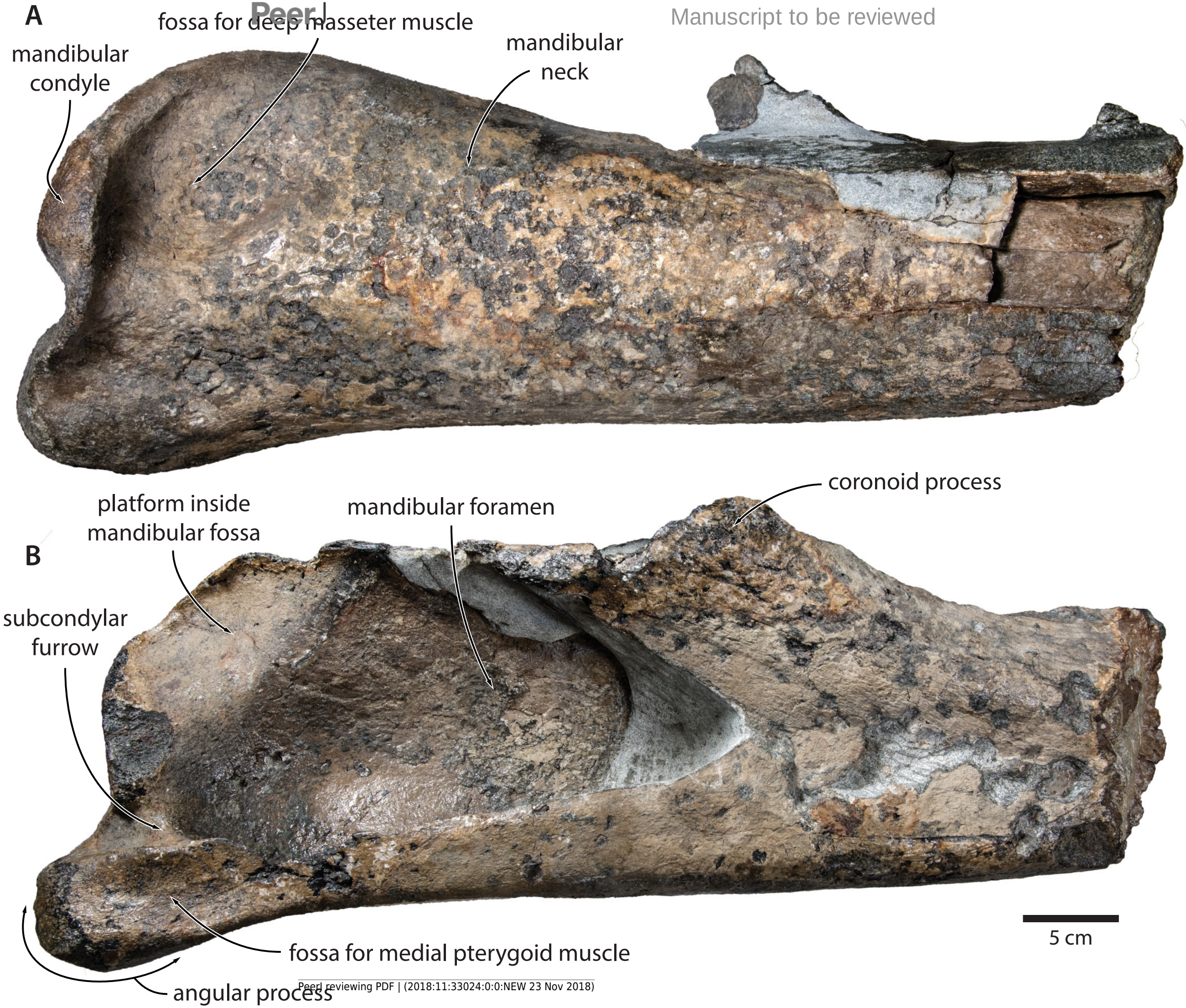
A
mandibular condyle
fossa for deep masseter muscle
mandibular neck
B
platform inside mandibular fossa
mandibular foramen
coronoid process
subcondylar furrow
fossa for medial pterygoid muscle
angular process
5 cm

Figure 9(on next page)

Comparison of the mandibular ramus of (A, C) *Tranatocetus maregermanicum* (NMR9991-16680, holotype) and (B, D) *Tranatocetus argillarius* (GMUC VP2319, holotype).

(A, B) medial, (C) lateral and (D) posterior view.

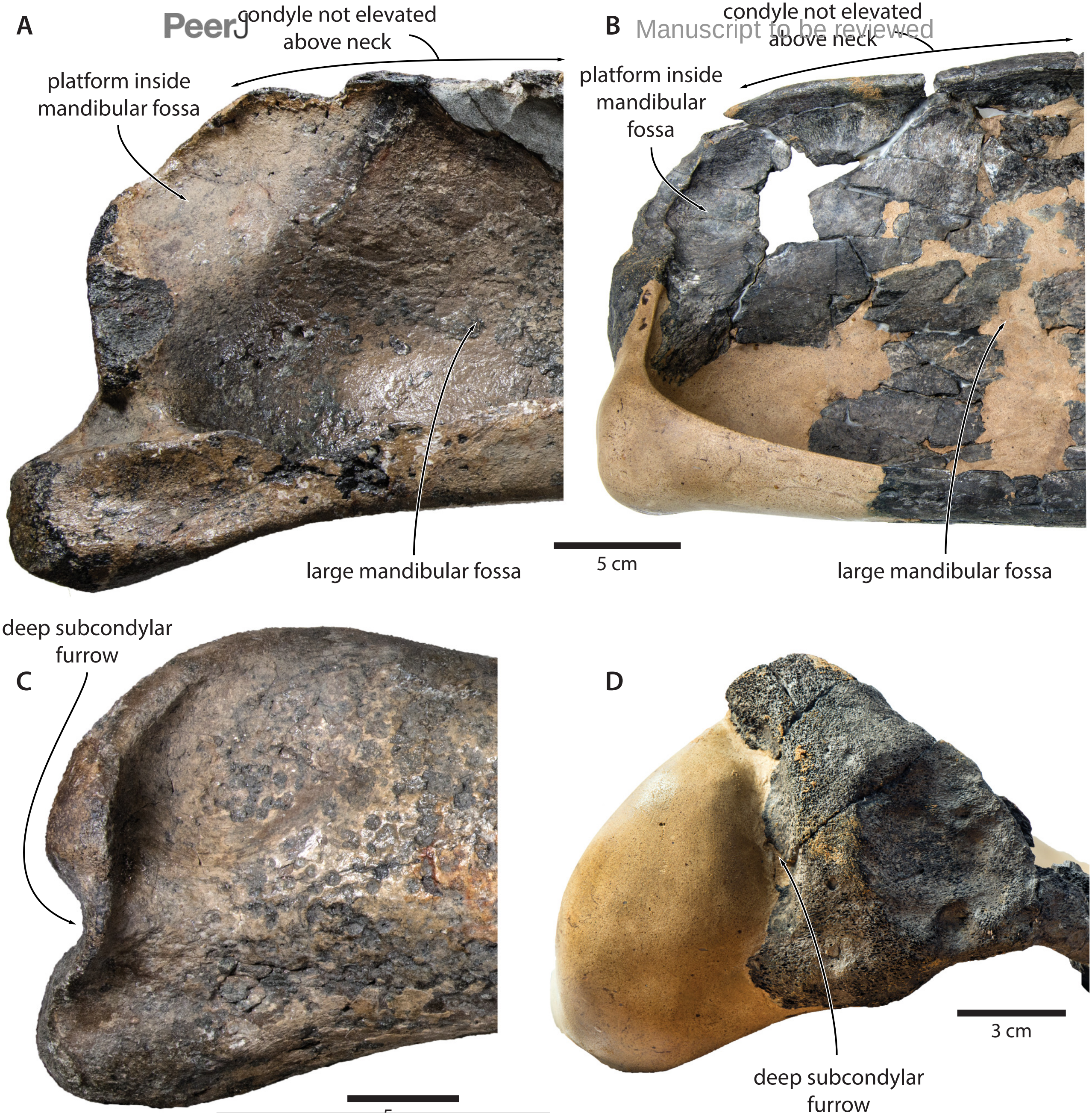
A
condyle not elevated
above neck
platform inside
mandibular fossa
large mandibular fossa
B
condyle not elevated
above neck
platform inside
mandibular
fossa
5 cm
large mandibular fossa
deep subcondylar
furrow
C
5 cm
D
3 cm
deep subcondylar
furrow

Figure 10(on next page)

Damage to the mandible and auditory region of *Tranatocetus argillarius* (GMUC VP2319, holotype).

Mandible in (A) anterior, (B) medial and (C) lateral view. (D) Auditory region in oblique right posterolateral view.

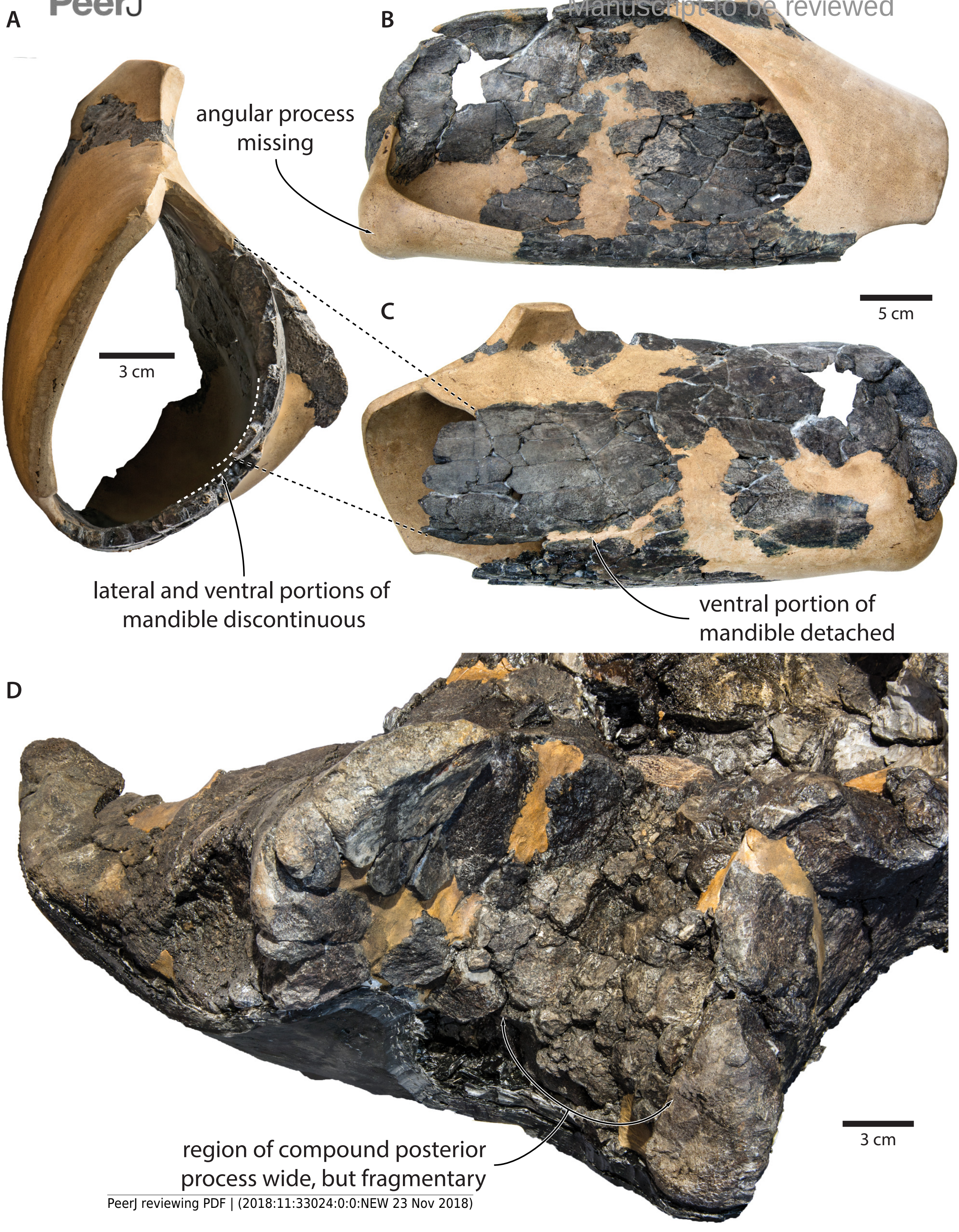
A
B
angular process missing
C
5 cm
3 cm
lateral and ventral portions of mandible discontinuous
ventral portion of mandible detached
D
3 cm
region of compound posterior process wide, but fragmentary

Figure 11(on next page)

Results of the total evidence phylogenetic analysis, showing the nesting of tranatocetids, including *Tranatocetus* itself, inside Cetotheriidae.

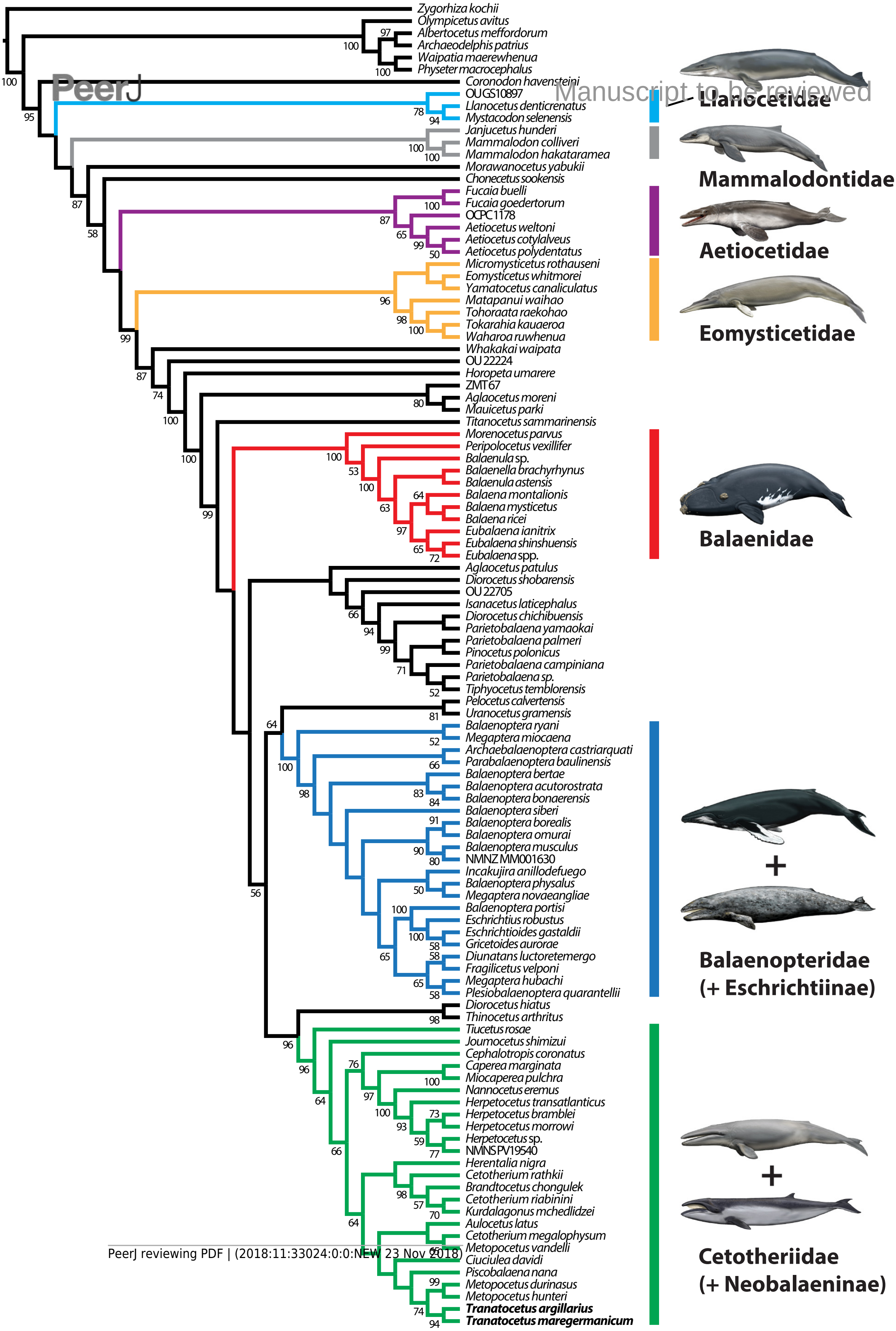
Zygorhiza kochii
Olympicetus avitus
Albertocetus meffordorum
Archaeodelphis patrius
Waipatia maerewhenua
Physeter macrocephalus
Coronodon havensteini
OU GS10897
Llanocetus denticrenatus
Mystacodon selenensis
Janjucetus hunderi
Mammalodon colliveri
Mammalodon hakataramea
Morawanocetus yabukii
Chonecetus sookensis
Fucaia buelli
Fucaia goedertorum
OCPC 1178
Aetiocetus weltoni
Aetiocetus cotylalveus
Aetiocetus polydentatus
Micromysticetus rothauseni
Eomysticetus whitmorei
Yamatocetus canaliculatus
Matapanui waihao
Tohoraata raekohao
Tokarahia kauaeroa
Waharoa ruwhenua
Whakakai waipata
OU 22224
Horopeta umarere
ZMT 67
Aglaocetus moreni
Mauicetus parki
Titanocetus sammarinensis
Morenocetus parvus
Peripolocetus vexillifer
Balaenula sp.
Balaenella brachyrhynus
Balaenula astensis
Balaena montalionis
Balaena mysticetus
Balaena ricei
Eubalaena ianitrix
Eubalaena shinshuensis
Eubalaena spp.
Aglaocetus patulus
Diorocetus shobarensis
OU 22705
Isanacetus laticephalus
Diorocetus chichibuensis
Parietobalaena yamaokai
Parietobalaena palmeri
Pinocetus polonicus
Parietobalaena campiniana
Parietobalaena sp.
Tiphyocetus temblorensis
Pelocetus calvertensis
Uranocetus gramensis
Balaenoptera ryani
Megaptera miocaena
Archaebalaenoptera castriarquati
Parabalaenoptera baulinensis
Balaenoptera bertae
Balaenoptera acutorostrata
Balaenoptera bonaerensis
Balaenoptera siberi
Balaenoptera borealis
Balaenoptera omurai
Balaenoptera musculus
NMNZ MM001630
Incakujira anillodefuego
Balaenoptera physalus
Megaptera novaeangliae
Balaenoptera portisi
Eschrichtius robustus
Eschrichtioides gastaldii
Gricetoides aurorae
Diunatans luctoretemergo
Fragilicetus velponi
Megaptera hubachi
Plesiobalaenoptera quarantellii
Diorocetus hiatus
Thinocetus arthritus
Tiucetus rosae
Joumocetus shimizui
Cephalotropis coronatus
Caperea marginata
Miocaperea pulchra
Nannocetus eremus
Herpetocetus transatlanticus
Herpetocetus bramblei
Herpetocetus morrowi
Herpetocetus sp.
NMNS PV19540
Herentalia nigra
Cetotherium rathkii
Brandtocetus chongulek
Cetotherium riabinini
Kurdalagonus mchedlidzei
Aulocetus latus
Cetotherium megalophysum
Metopocetus vandelli
Ciuciulea davidi
Piscobalaena nana
Metopocetus durinasus
Metopocetus hunteri
Tranatocetus argillarius
Tranatocetus maregermanicum
Llanocetidae
Mammalodontidae
Aetiocetidae
Eomysticetidae
Balaenidae
+
Balaenopteridae
(+ Eschrichtiinae)
+
Cetotheriidae
(+ Neobalaeninae)

Figure 12 (on next page)

Comparison of the auditory regions of (A, C) the presumed tranatocetid '*Cetotherium*' *megalophysum* (USNM 10593, holotype) and (B, D) the cetotheriid *Piscobalaena nana* (MNHN SAS 1616).

(A, B) Auditory region in ventral view. (C, D) Compound posterior process in (C) ventrolateral and (D) oblique posterolateral view.

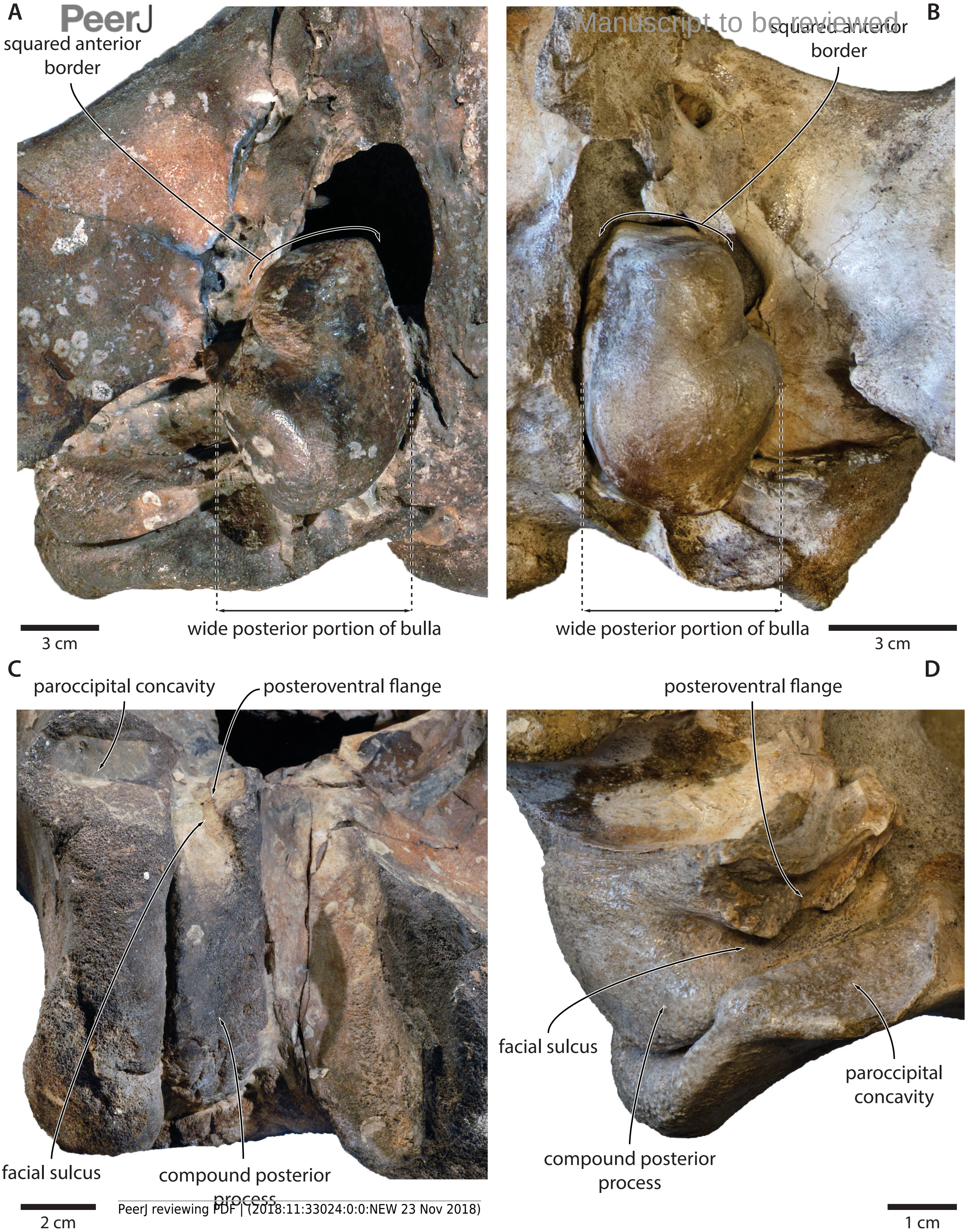
A
squared anterior
border
wide posterior portion of bulla
3 cm
B
squared anterior
border
wide posterior portion of bulla
3 cm
C
paroccipital concavity
posteroventral flange
facial sulcus
compound posterior
process
2 cm
D
posteroventral flange
facial sulcus
paroccipital
concavity
compound posterior
process
1 cm

Table 1(on next page)

Table 1 Measurements of *Tranatocetus maregermanicum* (in mm).

Table 1 Measurements of *Tranatocetus maregermanicum* (in mm)

NMR NMR9991-16680 (holotype)	
Bizygomatic width	860
Width across exoccipitals	590
Bicondylar width	190
Width of foramen magnum	81
Height of foramen magnum	54
Width across parietals at intertemporal constriction	130
Width of ascending process of maxilla (left)	48
Length of compound posterior process	107
Width of distal exposure of compound posterior process	75
Height of distal exposure of compound posterior process	40
Diameter of external acoustic meatus	34
Length of tympanic bulla	99
Width of tympanic bulla at sigmoid process	82
Width of atlas	224
Length of atlas	75
NMR9991-16681 (paratype)	
Bicondylar width	190*
Width of foramen magnum	60
Height of foramen magnum	70
Length of periotic (anterior process + body)	113*
Width of periotic	54
Height of periotic	43
Length of pars cochlearis	40
Width of pars cochlearis	24
Width of atlas	244*
Length of atlas	81
Height of atlas	180

* estimated